AN ABSTRACT OF THE THESIS OF

Da-Wei David Yu for the degree of Master of Science in Chemical Engineering presented on December 15, 1998. Title: Turbulent Pipe Flow Drag Reduction with Narrow Distribution Polystyrene Materials - A Test of Drag Reduction Theories

Abstract approved: _____

W. E. (Skip) Rochefort

The goal of the present studies is to test the "Time Scale" theories of the turbulent drag reduction in pipe flow with the use of dilute solutions of high molecular weight, narrow distribution polystyrene materials. The most important molecular parameter in the Time Scale theories is the maximum polymer relaxation time (τ_m). Therefore, it is important to have the well-characterized polymers for which τ_m can be unequivocally calculated.

The drag reduction experiments were conducted in a single-pass pipe flow apparatus using well-characterized polystyrene samples (TosoHaas Co.) in a good solvent (toluene) in the very dilute regime. The "Yo-Yo" theory proposed by Ryskin (1987) to predict the amount of drag reduction was also examined. Since the shear degradation is always an issue when using very high molecular weight polymers, shear degradation experiments were conducted by repeated passes through the pipe flow system.

In most of the broad distribution samples used in past studies, it has been suspected that a very high molecular weight tail has been present and the tail was responsible for a significant amount of the drag reduction. Thus, mixtures of the lower

molecular weight polystyrenes (MW=1 ~ 3.84×10^6) with the higher molecular weight polystyrenes (MW=20×10^6) have been studied to examine the effect of molecular weight distribution.

The results can be summarized as follows. The onset of drag reduction tends to occur at lower wall shear rate as the molecular weight of polymer is increased. The magnitude of drag reduction increases with increasing concentration. Ryskin's "Yo-Yo" theory was found to be deficient in accurately predicting the amount of drag reduction. The higher molecular polystyrene is more readily degraded in high shear conditions. The highest molecular weight component in the mixtures dominates both the onset and the drag reduction.

Moreover, the Time Scale theories predict that the onset is controlled by the Deborah Number (De) which is defined as $De = \tau_m \dot{\gamma}_w$, where $\dot{\gamma}_w$ is the wall shear rate. The present studies show that it is more appropriate to use the shear rate along the vortex lines of the turbulent eddies when calculating the De. When this is done, $De \cong 0.8 \sim 1.8$ are calculated at the onset point.

Turbulent Pipe Flow Drag Reduction with Narrow Distribution Polystyrene Materials - A Test of Drag Reduction Theories

by

Da-Wei David Yu

A THESIS

submitted to

Oregon State University

in partial fulfillment of

the requirements for the

degree of

Master of Science

Completed December 15, 1998

Commencement June 1999

Master of Science thesis of Da-Wei David Yu presented on December 15, 1998

APPROVED:

Major Professor, representing Chemical Engineering

Head of Chemical Engineering Department

Redacted for privacy

Dean of Graduate School

I understand that my thesis will become part of the permanent collection of Oregon State University libraries. My signature below authorizes release of my thesis to any reader upon request

Redacted for privacy

Da-Wei David Yu, Author

ACKNOWLEDGMENTS

As a foreign student coming from Taiwan, the two years of studying at Oregon State University have been an important time of my life. Fortunately, the time has been fulfilled due to the pleasure that I have when interacting with many great people. In particular, this research project can not be successful without the contributions given by certain people. Thus, it is now my turn to give the gratitude and praise to those who have helped me accomplish this project.

First of all, I would like to give the special thanks to my advisor, Dr. W. E. "Skip" Rochefort for the scholarly advice that is inspirational and valuable. I admire Skip for his profound knowledge of Polymer Science and Engineering. I have always felt pleasant to conduct this project under his professional instruction.

I appreciate the efforts of my committee members, Dr. Skip Rochefort, Dr. Goran Jovanovic, Dr. Philip Watson, and Dr. Gary Klinkhammer. They have been very helpful to me and have given their precious time to understand this project.

Uncountable thanks go to my parents who always encourage and support me at every step of my life. They really help me to concentrate on my study as they have established a "worry-free" atmosphere for me in these two years. The thanks are expanded to my younger brother for constantly giving me the confidence in a fraternal way, with which I would be able to overcome any challenges encountered.

I would like to show my appreciation to Su, Michelle, Dung, Michael, and Nelson, for being the staff while I was taking charge of Chinese Students Association at Oregon State University. They have always been and will always remain as the great friends of mine.

Lastly a special friend of mine, Joyce Chang, deserves my many thanks. Her gorgeous smiles and enlightening encouragement make me understand that the life is so beautiful.

TABLE OF CONTENTS

TABLE OF CONTENTS (Continued)

LIST OF FIGURES

LIST OF FIGURES (Continued)

LIST OF TABLES

LIST OF FIGURES (APPENDIX)

Turbulent Pipe Flow Drag Reduction with Narrow Distribution Polystyrene Materials - A Test of Drag Reduction Theories

CHAPTER 1
INTRODUCTION

It was Toms (1949) who reported in literature that minute amounts of added long-chain polymer could reduce the drag of solutions in a turbulent flow pipe. Although the effect of added polymer was earlier observed by Mysels and co-workers at Edgewood Arsenal in 1948 with use of aluminum soaps. Toms however, showed for the first time that minute amounts, 5-10 ppm per weight, of polymers could have a surprisingly tremendous effect. Ever since, drag reduction has received continuous attention through several decades even till now.

In addition to the great impact of drag reduction on turbulence it also has remarkable contributions in solving environmental problems and in achieving the more cost-effective industrial processes. For example, the Trans-Alaska Pipeline made advantage of drag reduction that is caused by the addition of polymers which increase the discharge without the construction of additional pumping stations. Therefore, the phenomena of drag reduction and the use of polymers as drag reducers were already known. Nevertheless, both were poorly understood. As a result, more studies on drag reduction are indeed required.

The studies carried out by Dick Nadolink (1987) investigated the drag reduction in a single-pass, pressure driven pipe flow system using well-characterized,

high molecular weight, narrow distribution polystyrenes in various organic solvents. His goals were to try to determine which of the proposed mechanisms for the onset phenomenon of turbulent drag reduction-- length, time, or energy-- was most appropriate (see Virk and Merrill (1969), Lumley (1973), or Zakin and Hunston (1980) for a review of the various onset theories) and try to explain how such small amounts of high molecular weight material could result in such large friction reductions. Ryskin (1987) incorporated elements from the work of several other researchers to propose an exciting newly developed theory, "Yo-Yo" theory, to quantitatively determine the drag reduction. The theory was checked using the experimental data of very high molecular weight polyacrylamide ($MW=2.0\text{-}2.5\times10^7$), but it had no attempt was made to characterize the samples. In this case, the agreement between Ryskin's theory and experimental data appeared inconclusive since a very large polydispersity normally exists in such a high molecular weight polymer.

This work was focused on the drag reduction involved with dilute well-characterized, high molecular weight, and narrow distribution polystyrene-toluene solutions in turbulent pipe flow. A main goal of the studies was to investigate the mechanisms underlying the drag reduction and onset phenomenon. Since the drag reduction and onset condition may vary greatly with molecular weight and concentration, the better understood mechanisms could help to determine the drag reduction and onset point for each concentration and molecular weight of interest. A second goal was to examine the "Yo-Yo" model by means of the experimental data obtained from the better characterized samples. A more accurate prediction for drag reduction in various

conditions was expected to be accomplished. Moreover, this work was to examine the Time Scale theories that were proposed to predict the onset of drag reduction.

CHAPTER 2
BACKGROUND AND LITERATURE REVIEW

2.1 Brief History

Drag reduction caused by dilute polymer solutions has been an area of continuous research for almost fifty years. There are probably many reasons for the relentless efforts on investigating the principles of drag reduction. But two of the main reasons must be the great potential for energy and cost savings with relatively little additional effort or equipment, and the elusive nature of the drag reduction mechanism, both in confined (pipe) and unconstrained (free turbulent jet) flows.

Experiments conducted the earliest by Toms (1949) and Mysels (1949) have established that the skin friction caused by turbulent flow of an ordinary solvent passing a solid surface could be reduced significantly by the addition of small amounts of certain materials to the solvent. Toms laid out a nice explanation for the drag reduction (DR) mechanism based on a time-scale argument and suggested that the primary mechanism of drag reduction could be the damping of small-scale eddies present in turbulent flow due to the molecular extension of additives and the subsequent increased viscosity. Since then, lots of studies have been done in this field trying to integrate new ideas for DR.

Virk (1975) presented an extremely complete review article which summarized most of the important work up to 1974, and the article heavily weighted with the studies of himself and his co-workers. Berman (1978) provided another much needed review with an emphasis of polymer physics and molecular models. His work has raised an question of whether or not drag reduction was a single molecule effect or intermolecular interactions, and has provided data on semi-rigid (DNA and collagen) and random coil (high molecular weight polyethyleneoxide) polymers.

Zakin and Hunston (1980) reviewed some of the unusual flow characteristics of drag-reducing solutions and discussed the effect of polymer molecular weight, concentration, solvency, and molecular weight distribution on drag reduction by using narrow distribution, and high molecular weight polystyrene samples. The discussion of various hypotheses on the onset of drag reduction was reviewed and compared with measured onset values in this article as well. K. Nakamura et al. (1988) have extended this work to investigate the effects of polymer concentration and solvent on the drag reduction efficiency in ultra-high molecular weight polystyrene ($MW=1.8\times10^7$) solutions using the rolling ball method.

Moussa and Tiu (1993) have reviewed numbers of studies on turbulent flow (shear) degradation of polymers and have used a capillary rheometer to investigate the effect of various parameters on polymer degradation in turbulent flow. These parameters included polymer concentration, contraction ratio, pipe length, pipe diameter, number of passes, solvent, and molecular weight of polymer. Moussa and Tiu suggested that most of the degradation took place at the entrance region of the pipe system.

However, numerous fine studies have already put significant efforts in this area so that trying to make a comprehensive review of the literature regarding drag reduction up to date is an all-consuming task to be done. To summarize the important literature that is related to drag reduction, a purposefully brief chronological sketch is given in Table 2.1.

Table 2.1 History of Turbulent Drag Reduction

1949	Toms (PMMA/monochlorobenzene) - 50% reduction in turbulent pipe flow
	Mysels (gasoline/aluminum soap) - U.S. patent 2,492,173 (12/23/49)
1959	Shaver and Merrill Dodge and Metzner - Non-Newtonian solutions (CMC)
1960's	Navy studies (Hoyt, Fabula, Ting, Hunston, Kenis....) - PEO (best DR at low concentration) - Catalogue of water soluble DR polymers
	Virk and Merrill - Maximum Drag Reduction Asymptote (random coil polymers)
1970's	DR Theories (Lumley, Virk, Walsh, Kohn, Metzner, Berman....) - Length, Time, and Energy theories - MODEL polymer systems (e.g., narrow distribution polystyrene)
1980's	Molecular dynamics in DR - Light Scattering and Birefringence studies - Heterogeneous DR (Berman....)
	Sellin, Hoyt, Pollert - Heat Transfer in Drag Reduction
	Zakin, Hunston, Nakamura, Nadolink - Effects of molecular parameters on DR - Onset point analysis
1991~	Moussa, Tiu, Sridhar - Polymer Degradation in turbulent flow
	Choi, Jhon - DR of PEO and oil-soluble polyisobutylene (PIB) in a rotating disk apparatus

2.2 Applications of Drag Reduction

Since the first few experiments in drag reduction caused by small amounts of polymers had been carried out, various applications based on this elusive concept of drag reduction were made. Some examples of successful commercial applications and possible future applications outlined by Hoyt (1972) and Bewersdorff (1995) are listed below:

- For fire department at New York City the pressure drop in a 700 ft long fire hose was reduced by 40% with the addition of 200 wppm of PEO to a pumper truck, resulting in a 50% increase in jet stream distance and a 10% increase in flow volume.
- Increased jet coherence at high flow rates has been applied to the development of water-based high speed drilling and cutting tools.
- Sellin and Ollis (1980) conducted studies on sewer system in England where they added the sewage flow with PEO and PAM. It was found that the flow rate increases of 60% for the same pressure head as solvent alone. In a full scale test on a 3 ft. diameter and 5 miles long sewer line they found drag reduction of up to 25%.
- The Navy has conducted sea trials on the 140 ft. coastal mine sweeper HMS Highburton, where they ejected PEO solution from slots in the bow (to ~ 10 wppm boundary layer concentration), resulting in ~ 13% speed increases at full power.
- The addition of small amounts of a very high molecular weight polymer (rumored to be polyisobutylene) to the crude oil flowing in the Trans-Alaska pipeline initially served as an emergency substitute for unconstructed pumping stations. It has been proved so successful that the dosing will continue and the pumping stations will have no need to be constructed.

- In primary flow circuits of large heating systems, in cooling flow circuits in the chemical industry, and in air-conditioning systems of large buildings the pumping energy could be reduced by the addition of drag reducers.
- For ship hulls, submerged bodies such as submarines, torpedoes and water-bourne rockets, and even for the swimmers, drag reducers were added into its turbulent boundary layer to produce drag reduction for those bodies in motion in a liquid.
- By using drag reducers, considerable energy saving could be achieved in the hydraulic transport of solids in pipes. That made hydraulic transport more economically attractive compared to transport by trucks, railways or ships.
- For human bodies, the addition of drag reducers into the blood could enhance the circulation of the blood and consequently reduce high blood pressure.
- Drag reducers which have no negative effects on the plants and on the soil could be added into the irrigation systems used in agriculture in order to increase the flow rate of the output. As a consequence, the production per area could be enhanced.
- Drag reducers working as stabilizing agents could be used to control the surface tension at the phase interfaces to maintain the geometry and stability of drops and bubbles.
- If cavitation near the wall occurs as the enormous pressure shocks increase due to the volume change of small bubbles of vapor generated by the local pressure declines below the vapor pressure. The addition of drag reducers is expected to reduce or to suppress the bubble formation since the additives lower the strain in the critical flow events. This interaction should reduce the size of the bubbles and increase their wall distance. As a consequence, the damages should be decreased in comparison to Newtonian fluids.

As was mentioned, these are just a few of the many applications on turbulent drag reduction that have been proposed so far. However, in general, more than 50 years of research on drag reduction has expanded the nature of basic studies into areas which include:

- Heat and Mass Transport
- Wall Roughness
- Stability of Laminar Flows
- External Boundary Layers
- Influences of Polymer Structure
- Normal Stress Effects
- Degradation of Polymer Molecules
- Anomalous Flows of Natural Polymers
- Vortex Inhibition
- Jet Coherence
- Drag Reduction of Soap and Fiber Suspensions

2.3 Drag Reduction Fundamentals

To help discuss drag reduction in dilute polymer solutions there are numbers of definitions and phenomena needed to be addressed. A typical friction factor versus Reynolds number plot for dilute, random coiling polymer solutions is shown in Figure 2.3-1 to make the discussion more straightforward. As shown in the plot, in the laminar flow regime (Re < 2100), for fully-developed flow the friction factor relates to the Reynolds number as the simple expression is given by,

$$f = 16/Re \qquad (2.3\text{-}1)$$

Figure 2.3-1 Typical Drag Reduction Plot for Dilute, Random Coiling Polymer Solutions

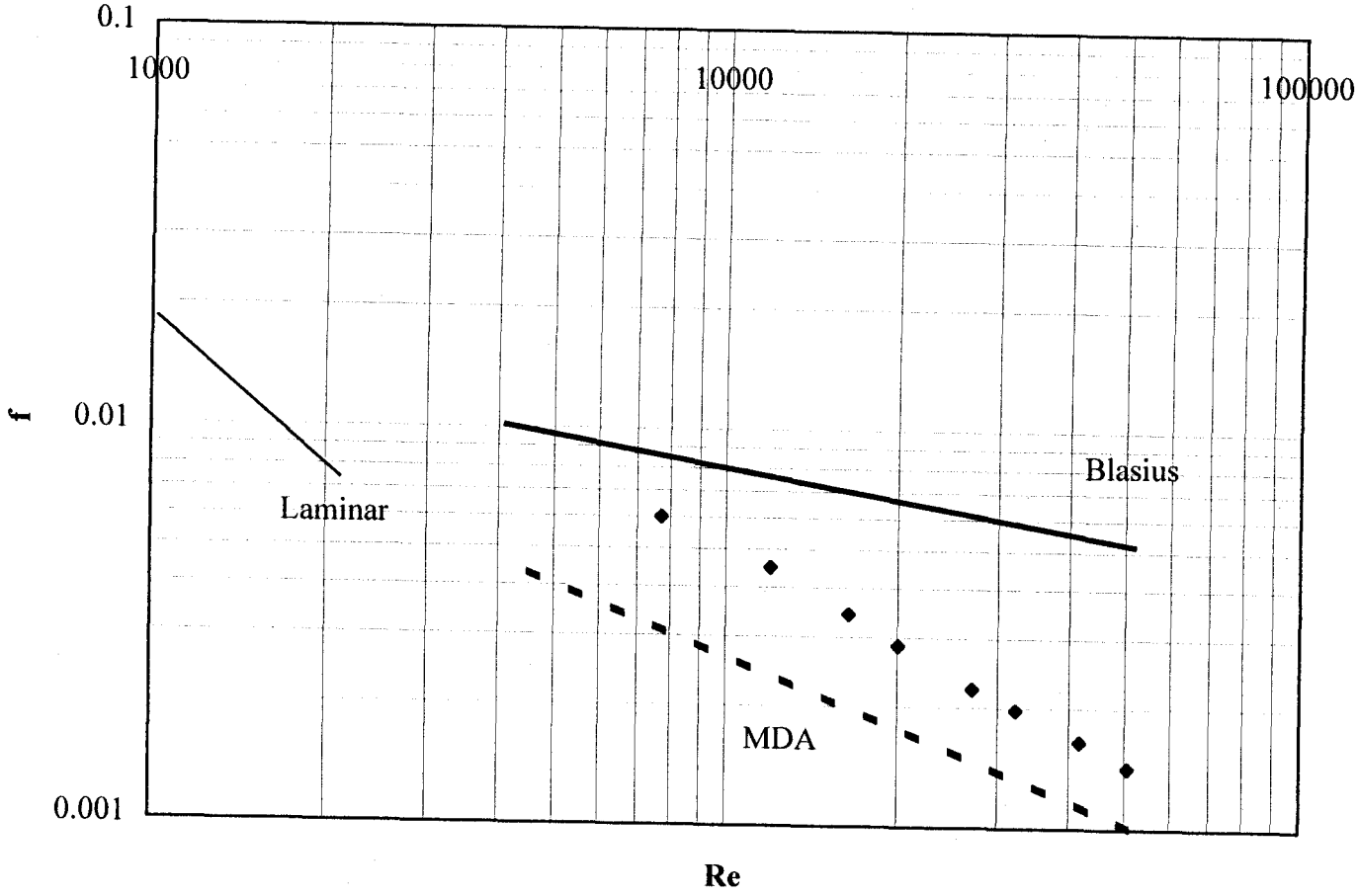

where the Reynolds number is defined as,

$$Re = \rho du/\mu \tag{2.3-2}$$

where ρ is the density of fluid, d is the diameter of the pipe, u is the fluid velocity, and μ is the fluid viscosity. The friction factor can be related to the pressure drop (ΔP) over a certain length (L) of pipe by the mechanical energy balance through the following equation,

$$f = \Delta P\, d/\, 2L\rho u^2 \tag{2.3-3}$$

In the turbulent flow regime (Re > 2100), the relationship between the friction factor and Reynolds number for Newtonian fluids in smooth pipes (solid line) is given by the Blasius expression (Davies, 1972),

$$f = 0.079Re^{-0.25} \tag{2.3-4}$$

The dotted line in the turbulent flow regime in Figure 2.3-1 is the so-called maximum drag reduction asymptote (MDA) which was developed by Virk (1970). MDA is an empirical equation that was developed by correlating a large number of data on random coiling polymers (mostly water soluble) and, consequently determining the maximum amount of drag reduction that could be obtained in a pipe flow, which is irrespective of polymer characteristics or concentration. The MDA in Prandtl-von Karman coordinates, which is another popular method of correlating turbulent drag reduction data (Davies, 1972), is given as,

$$f^{-1/2} = 19 \log (Ref^{1/2}) - 32.4 \tag{2.3-5}$$

and the Blasius expression in the Prandtl-von Karman coordinates is given by,

$$f^{-1/2} = 4 \log (Ref^{1/2}) - 0.4 \qquad (2.3\text{-}6)$$

There are many ways to present drag reduction data, but the f vs Re format and the Prandtl-von Karman format will be two main types used in these studies. The Prandtl-von Karman format of Figure 2.3-1 is shown in Figure 2.3-2.

The **onset** point of turbulent drag reduction is defined as the point where the friction factor measured for the polymer solution (f_p) first becomes lower than that measured for the solvent alone (f_s) at a specific Reynolds number. There are several proposed theories, based on length, time, or energy scales, predict the onset, but none has proven completely successful to date. More details about these theories will be described in the next section. According to the most popular time scale theories, onset is a function of molecular size or relaxation time (τ_m), and a characteristic turbulent time or length scale. As normally observed, the higher the molecular weight, the earlier the onset for random coiling polymer solutions. For a given molecular weight, the onset always occurs at the same wall shear stress (T_w) or shear rate ($\dot{\gamma}_w$). The wall shear stress is given by,

$$T_w = \rho u^2 f/2 \qquad (2.3\text{-}7)$$

and the equation used to determine the wall shear rate is expressed as,

$$\dot{\gamma}_w = T_w/\mu \qquad (2.3\text{-}8)$$

The amount of drag reduction (**%DR**) at a given Reynolds number is always defined as,

Figure 2.3-2 Prandtl-von Karman Format for Typical Drag Reduction Plot

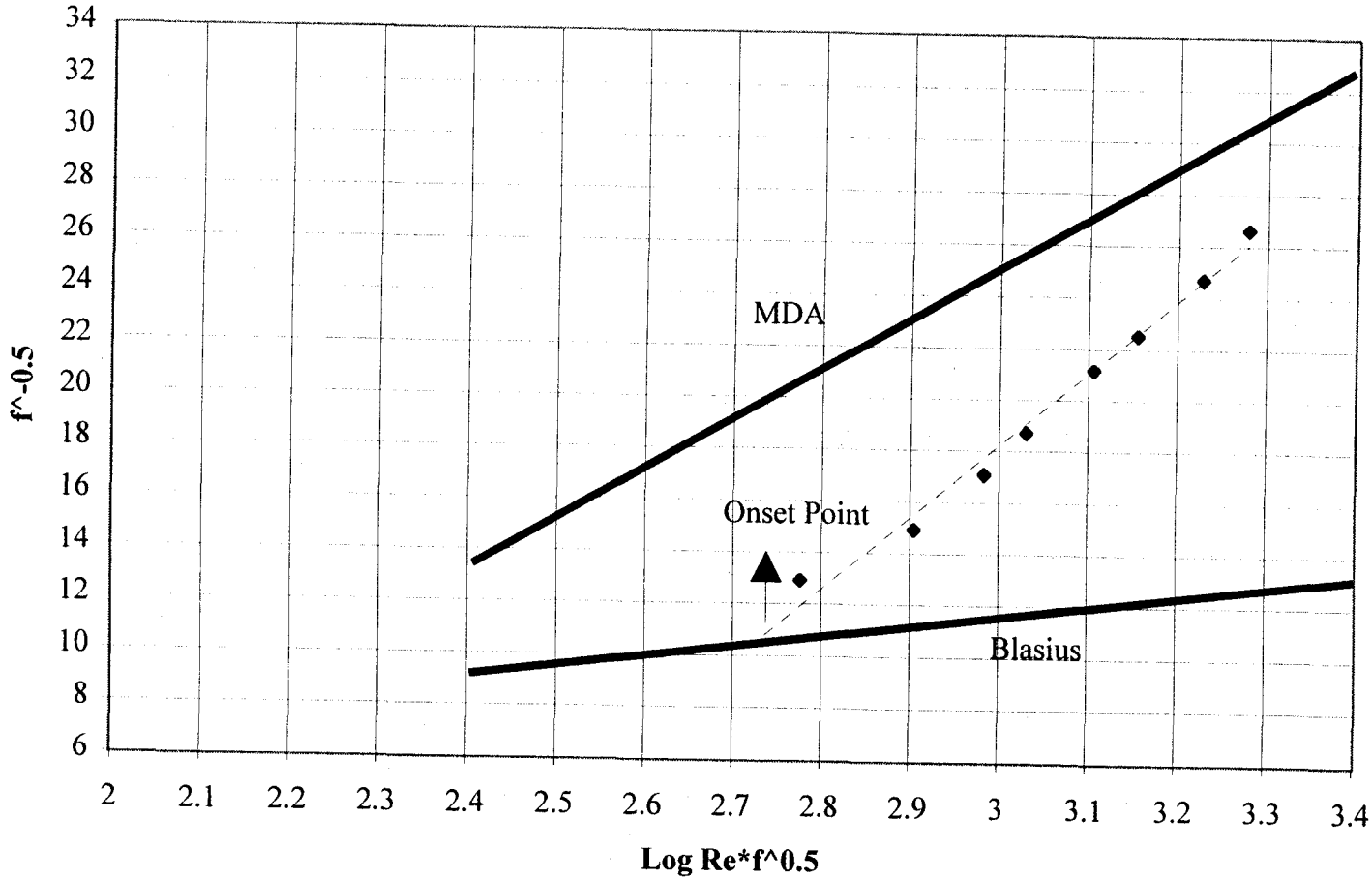

$$\%DR = [(f_p - f_s)/ f_s]* 100 = [(\Delta P_p - \Delta P_s)/ \Delta P_s]* 100 \quad (2.3\text{-}9)$$

and is essentially the difference between the pressure drop for the solvent (ΔP_s) and for the polymer solution (ΔP_p) at a given Reynolds number. In all cases, the %DR increases with concentration at the same molecular weight, and with the molecular weight at the same concentration, up to the MDA. However, the %DR increases with flow rate (Re) until the shear degradation of the molecule (decrease in molecular weight) occurs, which makes the %DR begin to decrease.

The maximum drag reduction asymptote (**MDA**) of Virk (1967) has been developed empirically for random coiling polymer solutions. It represents the maximum amount of drag reduction that can be obtained in a particular flow system, regardless of further increases in polymer concentration or molecular weight (i.e., once the combination of the two is sufficient to reach the MDA, further increases of either will result in no increase in %DR). Virk (1971) pointed out that it is not laminar flow, but instead represents the point where the elastic sublayer, in which the polymer molecules interact with the turbulent flow, has extended to the center of the pipe and thus no further turbulence damping is possible.

2.4 Drag Reduction Theories

Several theories have been established to predict the onset point and the amount of drag reduction in high molecular weight, dilute polymer solutions. It is important to note that all the theories are restricted to the solutions of $c << c^*$ (overlap concentration), where there is completely only single molecule behavior. In the following sections, Length, Time, and Energy scale theories are introduced and briefly discussed. A particular Time Scale theory that attracted popular support in the early 90's, the "Yo-Yo" theory, will also be discussed.

2.4.1 Length Scale Theories

The principal theory was proposed by Virk et. al. (1966), hence referred to as Virk's hypothesis. The theory claims that the onset of turbulent drag reduction occurs when the dimensionless ratio of the individual polymer length scale to the smallest turbulent length scale reaches an empirically determined constant. The relation is given by,

$$\Omega = (2R_g/\eta)(T_w^*/\rho) = 0.015 \qquad (2.4\text{-}1)$$

where R_g is the radius of gyration of a polymer molecule. Ω is the onset parameter, which was determined for a wide variety of random coil polymer solutions. However, Kohn (1973) revealed a poor correlation with Virk's theory when applying to a larger range of polymer molecular weights and concentrations. The key points about Virk's theory are that the theory predicts only onset, and is an interaction theory which relies on the compatibility of the polymer and flow length scales for an effect to be seen. The interaction theory does raise some controversy, since it does not physically satisfy to envision polymer molecules that interact with turbulent scales which are $10^2 \sim 10^3$ larger in the significant energy dissipation range. Nevertheless, with a semi-rigid or rodlike molecule, it might be feasible to replace R_g with L_c (the contour length) to make the concept much more practical.

2.4.2 Time Scale Theories

Several investigators, Elata (1966), Fabula (1967), and Hershey (1967), have pointed out that the onset should occur when the ratio of polymer to turbulent flow time scales is equal to unity. The relation is given by,

$$(\tau_m)(\dot{\gamma}_w^*) = M\eta_s[\eta]_0(\dot{\gamma}_w^*)/2.367RT \sim 1.0 \qquad (2.4\text{-}2)$$

where

$\dot{\gamma}_w^*$ is the onset wall shear rate

M is the polymer molecular weight

τ_m is the polymer terminal relaxation time (i.e., longest relaxation time)

η_s is the solvent viscosity

$[\eta]_0$ is the polymer-solvent intrinsic viscosity

R is the universal gas constant

T is the absolute temperature

The most commonly used relaxation time is given by the Zimm (1956) theory as shown in (2.4-2). It is known that Zimm theory describes the molecular behavior in "poor" solvents better than in "good" solvents However, using Zimm theory to predict the relaxation time in polymer solutions still remains feasible though small deviations may be observed in good solvents.

The Time Scale theory predicts only onset and is an interaction theory, but the concept of a flexible long chain molecule interacting with a fluctuating flow field is more physically satisfying. In fact, if the burst-lift-sweep mechanism of turbulent production (Bremhorst and Walker, 1973) is envisioned so that turbulence can be considered as a "strong" flow. The Deborah number ($De = \tau_m\dot{\gamma}_w^*$) will show a significance because large increases in elongational viscosity are predicted to occur at De = 0.5 by dilute solution molecular theories (Bird et. al, 1977). This accidentally supports the assumption made by Lumley (1973), that the increase in the elongational viscosity is the primary mechanism for drag reduction. However, Kohn (1977) and Zakin et. al., (1980) observed a poor correlation of onset data compared to the Time Scale theory as their experimental

data of De were one order of magnitude larger than the value predicted by Time Scale theories.

Many researchers have studied the role of elongational viscosity of drag-reducing solutions in turbulent flow. Durst et. al. (1982) have modeled both laminar flow in porous media and turbulent pipe flow with an interesting physical model to study the effect of elongational viscosity and describe the effect of polymer additives. As shown in Figure 2.4-1a the model of the turbulent flow field as counter-rotating eddies is used to depict the extensional flow field envisioned. If the flow field is strong enough, the molecule will begin to extend. This causes an increase in the extensional viscosity, and consequently causes an increase in the resistance to flow. Therefore, in the case of porous media flow, an increase in the pressure drop is observed. In Figure 2.4-1b the finitely-extensible, non-linear elastic (FENE) dumbbell model predicts the elongational viscosity as a function of De (Bird et. al., 1977), and shows large increases in viscosity for De > 0.5. Figure 2.4-1c is a plot of the elongation strain rates as a function of the position across the pipe. Incorporating the results of Figure 2.4-1b, one can use the plot to describe the region in the pipe where the polymer should be effective. As can be seen, a larger relaxation time will result in a greater area experiencing a strain rate that is large enough to significantly increase the elongational viscosity. Thus, the increased elongational viscosity will damp the turbulent eddies resulting in a greater drag reduction. In summary, this model provides a physical interpretation of the Deborah number arguments (i.e., large increases in elongational viscosity) based on dilute solution molecular theories with the flow in the pipe.

2.4.3 Energy Theories

Two principal energy theories have been developed so far. The first theory by Walsh (1967) proposed that onset occurs when the ratio of the rate of energy storage by

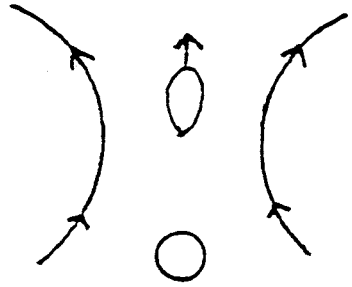

Figure 2.4-1a Molecular Deformation between Counter-Rotating Eddies

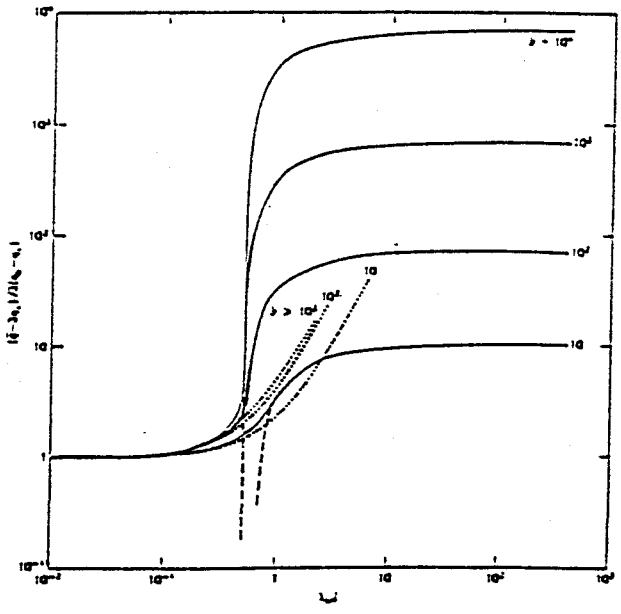

Figure 2.4-1b Elongational Viscosity Curves for FENE Dumbbell Model (Bird et. al., 1977)

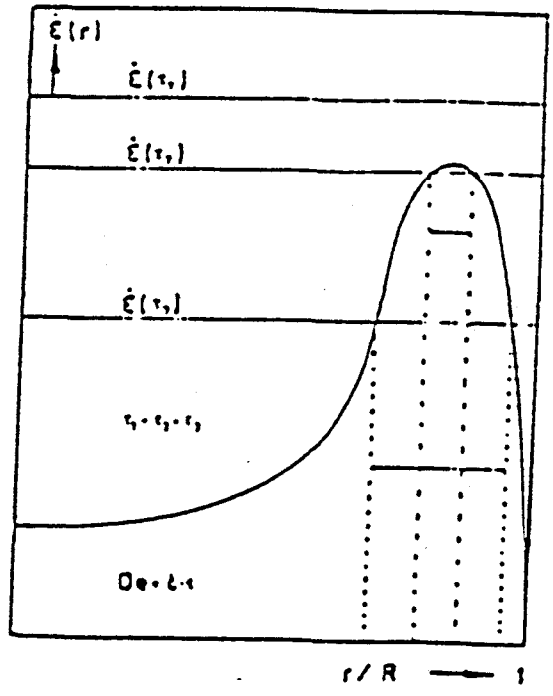

Figure 2.4-1c Elongation Strain Rates across the Pipe
(Durst, Hass, and Interthal, 1982)

polymer molecules to the rate of convection of turbulent energy away from the wall exceeds 0.01. The relation is shown as,

$$H = 8CM(\eta)^2 T_w^*/RT > 0.01 \qquad (2.4\text{-}3)$$

Furthermore, when $H \rightarrow 1.0$, significant amounts of energy which would have been convected away by turbulent bursting disturbances would be stored in the deformation motions of the polymer molecules, indicating that the effect would be maximized for a given polymer/solvent system. Again, this idea is physically satisfying and going beyond the pure onset theories. But Kohn (1973) has shown that it is a poor correlation of general data.

Kohn (1973) has derived an expression for the energy stored by the polymer molecules exposed to a fluctuating wall shear rate. The term is called strain energy density and has its origins in the theory of rubber elasticity. Kohn argued that polymer molecules need only to be stretched in the flow direction 2-3 times their unperturbed dimensions to have the ability of storing energy under high shear conditions and dissipating the energy when relaxed in a low shear field. This mechanism allows for the decreased production of energy as compared to pure solvent flow, and relies only on the polymer's ability to store energy, and not on the rate of convection of turbulent energy as Walsh's theory holds. The strain energy density is given by,

$$W = (CRT/2M) \sum_{1}^{N} \ln [1 + (\dot{\gamma}\, \tau_i)^2] \qquad (2.4\text{-}4)$$

where W is the strain energy density (erg/ml), N is the number of statistical segments per molecule in a bead-spring model, and τ_i is the relaxation time of the ith mode. The appeal of this model is physical, but it is difficult to implement, particularly for the polymers which are not model systems (i.e., not narrow MWD or well-characterized).

Besides these above-mentioned models, one model which is most often quoted and provides an interesting conceptual interpretation of the drag reduction phenomenon was proposed by Virk (1971). The model is called the Elastic Sublayer Model. As was mentioned in a previous section, Virk correlated a large amount of experimental data on random coil polymers and achieved a maximum drag reduction asymptote (MDA). The plot shown in Figure 2.4-2 is taken from Virk (1970). Virk then replotted the equation for the MDA line in the classic Law of the Wall coordinates ($u^+ = U/u_t$, $y^+ = y\ (u_t/\nu)$; Davis, 1972), and added some other experimental data in at various intermediate levels of drag reduction. He observed that there was a parallel upshift relative to the solvent at low levels of DR with a tendency towards the MDA as DR increased (as shown in Figure 2.4-3). Purely based on the experimental evidence, he claimed that the mean velocity profile is composed of three segments (Figure 2.4-4). The segments, if proceeding from the pipe wall to the pipe center, are: 1) a viscous sublayer (Newtonian); 2) an interactive zone which he called the elastic sublayer as a characteristic of drag reduction; 3) an outer region (Newtonian plug). The most important zone in this model is the elastic sublayer where all the polymer effects are assumed to occur. Figure 2.4-5 shows the relationship between the three different regions and the Law of the Wall coordinates. The extent of DR relies solely on the location of the outer edge of the sublayer, y_e^+, and drag reduction increases as y_e^+ is approaching R^+, at which point the MDA is reached. At intermediate levels of DR, the velocity profile displays an "effective slip" in which the Newtonian turbulent core is parallel-shifted upward to solvent. Since the model is consistent with experimental data in the intermediate region, this provides a good physical description of one way to visualize the drag reduction phenomenon.

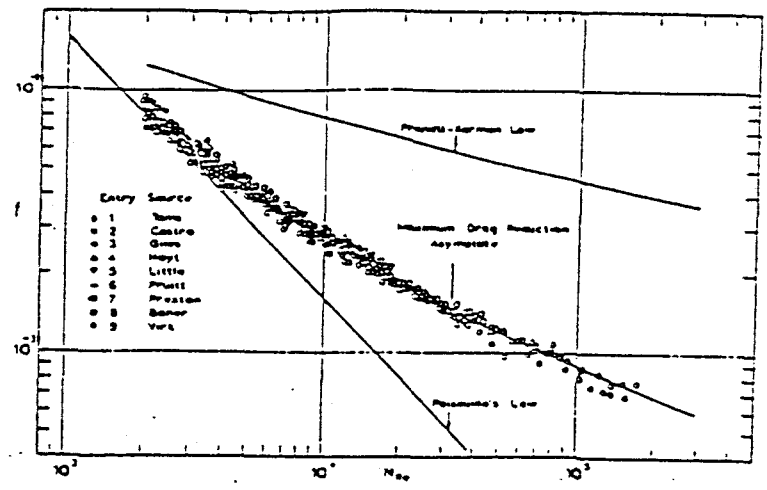

Figure 2.4-2 f vs Re plot of Maximum Drag Reduction Asymptote (MDA) for Random Coiling Polymers (Virk, 1970)

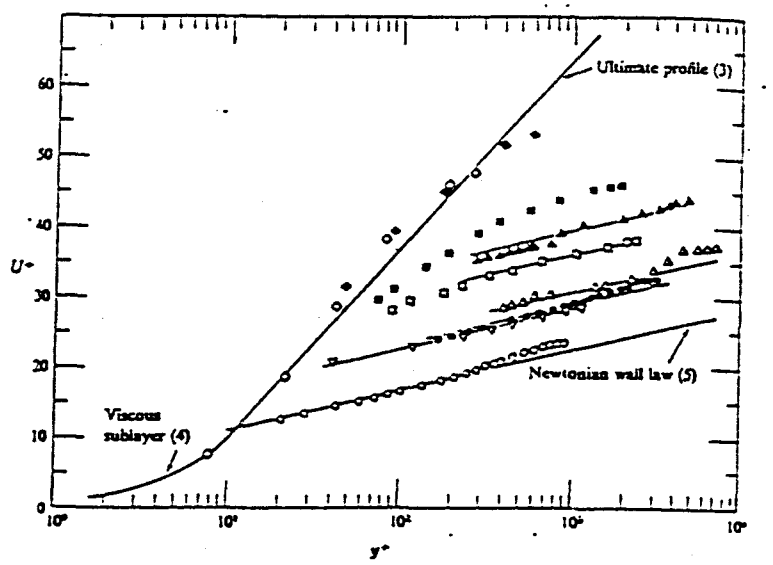

Figure 2.4-3 Law of the Wall plot for Random Coiling Polymers (Virk, 1971)

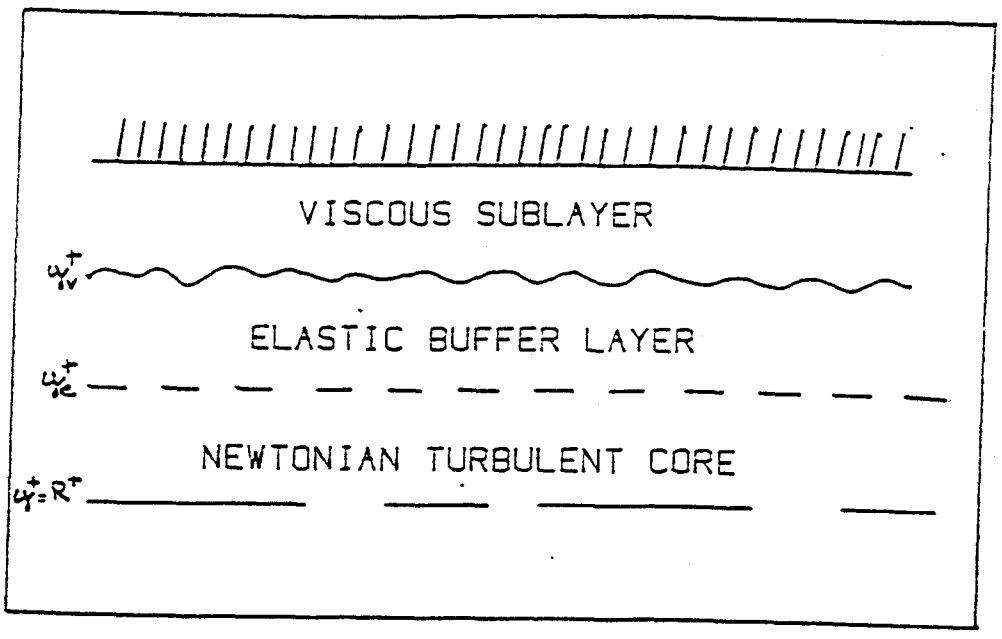

Figure 2.4-4 Outline of the Elastic Sublayer Model (Virk, 1971)

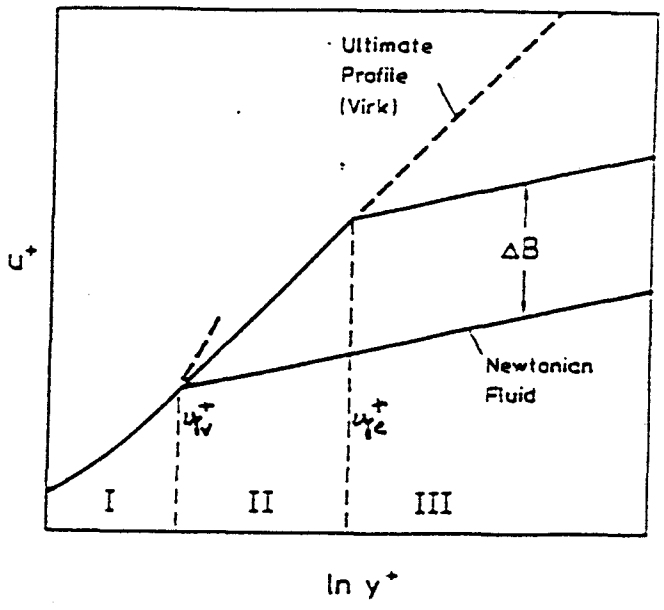

Figure 2.4-5 Schematic of the Law of the Wall in the Elastic Sublayer Model. (I) Viscous Sublayer (II) Elastic Buffer Layer (III) Newtonian Turbulent Core. ΔB = Effective Slip

2.5 Ryskin's "Yo-Yo" Theory of Drag Reduction

Perhaps the most recent quantitative theory to predict drag reduction was presented by Ryskin (1987). In this theory, the effective viscosity increase in turbulent flow caused by the unraveling molecules is calculated, and a relationship between the viscosity increase and the drag reduction is also presented. He proposed that the polymer chain unravels during stretching in an elongational flow field if the strain rate exceeds a critical value, such that the central portion of polymer chain becomes straightened while the both ends that move apart remained coiled. If the flow later becomes weak, the chain can curl back upon itself. Due to the obvious configuration, Ryskin termed this physical interpretation a "Yo-Yo" model.

However, Ryskin's theory is not original but rather it incorporates elements from the work of other researchers. Following the original paper by Ryskin (1987), a description of how Ryskin applied his "Yo-Yo" model to past theories, and a derivation of the resulting equations which allow one to quantitatively predict DR in turbulent pipe flow are given below.

At very low strain rates, a polymer molecule in dilute solution will be present hydrodynamically as a sphere of radius R_0. As the strain rate in an elongational flow increases, the viscous forces will keep the molecule elongating until they are balanced by an entropic restoring force. The extent of the restoring force is proportional to the amount of the deformation of the sphere, i.e., $(l-2R_0)$, where l is the effective length of the fully extended polymer chain. The viscous force increases with l to a power ε, where ε is close to 2 at large elongation. Thus, there must exist a critical strain rate, γ_{cs}, and a critical length, l_{cs}, past which the viscous force will dominate and the stretching will become a runaway process until the molecule extends to its full length. The balance between the viscous force and the entropic restoring force is given by,

$$C_1 l_{cs}^{\varepsilon} = C_2(l_{cs}-2R_0) \tag{2.5-1}$$

using equation (2.5-1) and its derivatives, an expression for the prestretching ratio can be obtained as,

$$\beta = l_{cs}/2R_0 = \varepsilon/(\varepsilon-1) \tag{2.5-2}$$

as mentioned previously, ε approaches 2 for large elongation. Thus it is expected that β is equal to 2. Theoretically, β is found to be 1.8 by Rabin (1983).

Ryskin argued in his model that the end coils have no significant contribution to energy dissipation of the flow, it is the center of the molecule which acts like a taut string that will increase the extensional viscosity of the fluid. Batchelor's theory for the stress in a suspension of rigid rods was used to determine the extent of the viscosity increase, ϕ, which is given by,

$$\phi = \pi n l^3/9\log(\pi/v) \tag{2.5-3}$$

where v is the hydrodynamically effective volume concentration of polymer and n is the number density of molecules ($n = CN_a/M$). Using Einstein's result for the effective viscosity of a dilute suspension of spheres, which is expressed as,

$$v = 4/3\pi R_0^3 n = 2/5C[\eta] \tag{2.5-4}$$

combining equations (2.5-2), (2.5-3), and (2.5-4), one can get

$$\phi = \kappa C[\eta]\xi^3 \tag{2.5-5}$$

where $\kappa = 4\beta^3/15\ln(5\pi/2C[\eta])$

$\xi = l/l_{cs}$ = instantaneous relative elongation of the molecule

Ryskin took the value of κ as a constant 0.3 in his model, since he claimed that κ is a very weak function of $C[\eta]$. In fact, this may not be a good idea because the concentration always varies by orders of magnitude in typical drag reduction experiments and $[\eta]$ also varies with molecular weight of the polymers.

When the molecule is fully extended, the value of ξ corresponds to ξ_{max}, which is defined as,

$$\xi_{max}=L/4R_0 = \frac{1}{4}[10\pi N_a M^2 a^3/3M_0^3[\eta]]^{1/3} \qquad (2.5\text{-}6)$$

where $L = Na$ = contour length of the polymer chain

N = degree of polymerization

a = stretched length of a repeat unit

$M_0 = M/N$ = molecular weight of a repeat unit

As stated previously, stretching becomes a runaway process, and continues the process until the molecule approaches its maximum dimension once the chain is elongated past a critical length. Besides, the strain rate needed to keep the chain extended is only a part of the strain rate that is required to elongate the chain originally. Ryskin proposed that in turbulent flow the molecule has a characteristic dimension which is some fraction of the maximum extended length. The relationship is given by,

$$\xi_{turb} = \alpha\xi_{max} \qquad (2.5\text{-}7)$$

Eventually, from equations (2.5-5), (2.5-6), and (2.5-7) one can get

$$\phi_{turb} = \kappa\alpha^3 5\pi N_a M^2 a^3 C/96M_0^3 \qquad (2.5\text{-}8)$$

where $(1+\phi_{turb})$ is the ratio of the instantaneous effective fluid viscosity of the polymer solution to that of the solvent.

In order to find the relationship between the viscosity increase and some quantitative characteristic of the drag reduction, the classical Prandtl's resistance law for a Newtonian turbulent pipe flow is first recalled,

$$f^{-1/2} = 2 \log (Ref^{1/2}) - 0.8 \qquad (2.5\text{-}9)$$

On the other hand, Virk (1975) found that the turbulent flow of a drag-reducing solution was of the form,

$$f^{-1/2} = (2+\delta)\log (Ref^{1/2}) - 0.8 - \delta \log(Ref^{1/2})_{onset} \qquad (2.5\text{-}10)$$

where δ is defined as the slope increment and its value is easily determined from a Prandtl-von Karman plot, in which δ is simply the difference in the slopes of the lines representing the Newtonian and drag reducing fluids. It is noted that the δ in Ryskin's theory is one-half that of Virk's.

Ryskin argued that the two constants 2 and -0.8 in (2.5-10) are of different natures- the first is "purely inertial" (independent of rheology), while the second depends upon the thickness of the viscous sublayer. This means that if in a polymer solution flow the wall shear stress are equal to the product of the velocity gradient at the wall and the effective viscosity, η_{turb}, then the resulting hypothetical friction factor, f_{turb}, would satisfy

a resistance law similar to (2.5-9) except that the constant -0.8 would be different. The relation between f_{turb} and f is, apparently, $f_{turb} = (\eta_{turb}/\eta_s)f$. Thus,

$$(\eta_{turb}/\eta_s)^{-1/2} f^{-1/2} = 2\log(Ref^{1/2}) + \text{constant} \qquad (2.5\text{-}11)$$

where the constant term includes all additive terms. Therefore $2+\delta = 2(\eta_{turb}/\eta_s)^{1/2}$ and as a result,

$$\delta = 2(1+\phi_{turb})^{1/2} - 2 \qquad (2.5\text{-}12)$$

In order to determine δ which in turn leads to predict the magnitude of drag reduction, ϕ_{turb} is expected to be calculated from (2.5-8) knowing α and other simple molecular information of a specific polymer.

Attempting to check the agreement between the predictions of the theory and experiments, Ryskin used the experimental results which were taken from Oliver (1983) for very low drag reduction caused by a commercial polyacrylamide material. In this case, α was found to be 0.23 to make his model exactly fit the experimental data. On the other hand, for the polymers with methylene, oxyethylene, and siloxane backbones (Virk), the experimental results fit in his model if α is equal to a constant 0.18.

The polyacrylamide materials which gave the experimental results for Ryskin to check his model were very high molecular weight polymers (MW ~ 20×10^6). However, there was no attempt made to characterize the polymers. Normally, a very large polydispersity is expected in the commercial polymers with such high molecular weight. On the basis of the polydispersity, the agreement between Ryskin model and experimental data truly appears inconclusive.

2.6 Polystyrene

Polystyrene is certainly not a classical drag reducing polymer, primarily due to its insolubility in water, which is the most common medium for drag reduction applications. However, in a good solvent (toluene) it is a very effective drag reducer at relatively low concentrations for molecular weights higher than two million. As early as 1969, Lumley proposed the need for applying well-characterized monodisperse polymers to build up more specific information about drag reduction, rather than employing the highly polydisperse polymers with which the majority of experiments had been conducted.

For a number of reasons, the polymer of choice became polystyrene. Over the past several years, samples of high molecular weight, narrow distribution polystyrene materials have been commercially available from manufacturers such as TosoHaas and Pressure Chemical. These materials are typically used as calibration standards for gel permeation chromatography. Thus they are also extremely well-characterized with respect to molecular weight and molecular weight distribution.

However, there are some drawbacks in using polystyrene as drag reducer as well. First, despite polystyrene is commercially available with good characterization, the cost of polystyrene is relatively high. Due to the high cost, the sample sizes in the drag reduction experiments are restricted. Second, polystyrene is only soluble in some organic solvents which are harmful to the environment. Thus it requires extra care to re-collect the solutions or even re-use the solutions. The third problem is that the organic solvents are also able to chemically attack a few parts in the pipe-flow apparatus, i.e., O-rings. As a result, extra care of doing more regular maintenance of pipe-flow apparatus is essential as well.

By testing the monodisperse polystyrene samples in drag reduction experiments, it is expected to clarify the role of molecular weight and molecular weight distribution in drag reduction.

CHAPTER 3
EXPERIMENTAL

This chapter will describe the preparation and characterization of the drag reducing solutions that were used to conduct the experiments, and the single-pass pipe flow system that was used for the experiments.

3.1 Solutions for Drag Reduction Studies

3.1.1 Preparation of the Polymer Solutions

The solutions that were made by dissolving polystyrene samples of varying molecular weight and concentration in toluene were used in drag reduction studies. The intention of this work to focus on polystyrene has been discussed in great detail in previous chapters. To be studied in this work, six monodisperse polystyrene samples were obtained: 1) PSF-128 (TosoHaas Co.), 2) PS-14A (Pressure Chemical Co.), 3) PSF-380 (TosoHaas Co.), 4) PSF-550 (TosoHaas Co.), 5) PSF-850 (TosoHaas Co.), and 6) PSF-2000 (TosoHaas Co.). They were termed as monodisperse because the ratio of Mw/Mn of each sample was less than 1.2. Polystyrene solution was prepared at room temperature by adding the appropriate weight of fine polystyrene powders very slowly and gently to a certain volume of toluene in a 4-liter beaker to achieve a particular concentration of interest using only a hand stirring rod. When the powders were entirely exhausted and well dispersed throughout the beaker, stirring was continued by using a magnetic mixing element at very low speed for 30 minutes. The solution was then allowed to stand in a tightly sealed brown bottle for 24 hours to complete dissolution of

the polystyrene sample. Just before the solution was to be tested in the single-pass flow system, solution was again stirred very gently with a stirring rod.

In the turbulent flow tests, the concentration was increased from the lowest value to the highest value in order to prevent from the concentration problems and the build-up in the apparatus. This procedure allowed for the most accurate maintenance of concentration and as well the easiest procedure because the complete flushing operation can be avoided between each new concentration test. The entire Reynolds number series was obtained at one sitting (from low to high) with each concentration.

3.1.2 Measurements of Viscosities of the Polymer Solutions

The viscosity of each polymer solution was measured using standard capillary viscometry. This was done to both determine the polymer molecular weight from the intrinsic viscosity measurements to compare to these reported by the manufacturers, and to test for possible shear degradation of the high molecular weight polymers during the drag reduction experiments.

The viscosity of polymer solution is always higher than that of the pure solvent, and is a function of temperature. The relative increase in the viscosity of the solvent as a result of dissolved polymer is called the specific viscosity of the solution, that is defined as shown below:

$$\eta_{sp} = \frac{\eta - \eta_s}{\eta_s} = \eta_{rel} - 1 \qquad (3.1\text{-}1)$$

where η is the solution viscosity, η_s is the solvent viscosity, and η_{rel} is the relative viscosity. Specific viscosity increases with the concentration of added polymer in the solution. Using the specific viscosity per unit concentration (i.e., η_{sp}/c) as a measure of

molecular weight of polymer was originally proposed by Staudinger (1930). The quantity of η_{sp}/c is called the reduced viscosity and its unit coincides with that of the concentration. As was done in this work, a graphical method is used to plot η_{sp}/c and ln η_{rel}/c as a function of concentration.

When the polymer solution is dilute (i.e., C→0), the value of η_{sp}/c approaches to a certain number that is defined as $[\eta]$. The equation is shown as,

$$\lim_{c\to 0} \eta_{sp}/c = [\eta] \tag{3.1-2}$$

The value of $[\eta]$ which can be obtained by the extrapolation of η_{sp}/c data to c = 0 is known as the intrinsic viscosity. Its unit depends upon the concentration. The empirical relationship between the intrinsic viscosity and the molecular weight of the polymer is governed by the type of solvent and temperature. In this work, the Mark-Houwink-Sakurada (MHS) equation was applied:

$$[\eta] = kM^a \tag{3.1-3}$$

where a ranges from 0.5 to 0.8 and depends on the polymer-solvent interaction. For good solvents, in which the polymer is freely dissolved, a = 0.6 ~ 0.8. For poor solvents, a decreases to the value of 0.5.

The molecular weight calculated by using specific viscosity data is the viscosity-average molecular weight, M_v:

$$[\eta] = \lim_{c\to 0} \eta_{sp}/c = KM_v^{\ a} \tag{3.1-4}$$

In order to obtain very accurate values of K and a for solutions, it is necessary to conduct a fractionation, and experimentally measure [η] of each fraction. If a remains constant over the range of fractionated molecular weights, log[η] will be a linear function of logM; the slope of the line is the value of a, and its intercept with the axis is equal to logK. The values of K and a and their constancy depend strongly upon the molecular weight distribution, the degree of polydispersity of the whole solution and the individual fractions, and on the method that is used to measure individual fractions. However, many works to determine the values of K and a for various polymer-solvent combinations have been completed so far and those works provide the accurate numbers of K and a for each different combination.

The reduced, and intrinsic viscosity measurements were made using a Cannon-Ubbelohde type capillary dilution viscometer (#75) at ambient temperature. For the measurements, the largest error was encountered with the timing of the falling solution column which was accomplished with a stop watch accurate to 0.01 second. The polymer solutions used in viscosity measurements were prepared as the same way as indicated in previous section. It is noted that, for viscometry measurements, the starting concentration of each polymer solution was always chosen as little below the overlap concentration of solution. The reason is that the interactions between polymers exist above the overlap concentration and as a result, the linear relationship between log[η] and logM is no longer present.

Finally, the measurements were carried out for all polystyrene samples which were to be used in this work in combination with toluene at ambient temperature (see Appendix). A straightforward dilution process was applied, in which the starting concentrations of solutions were cut by a factor of two in each succeeding run until enough points were collected to find a least-squares fit to both viscosity relations. As a result, a concurrent mutual intersection at zero concentration can be found, which was defined as the intrinsic viscosity, [η]. The results helped to derive not only the viscosity-

average molecular weight of each polystyrene sample but also the subsequent calculations of terminal relaxation time for each polystyrene samples in drag reduction experiments.

With the use of polystyrene samples in this work, the following is the equation which was applied in the viscometry measurements to calculate the viscosity-average molecular weight of polystyrene samples,

for polystyrene in toluene at 20^0C,

$$[\eta] = KM_v^a \tag{3.1-5}$$

where $K = 4.16\times10^{-3}$ ml/g, and $a = 0.788$.

The characteristics of the polystyrene samples used in this work are listed in Table 3.1.

Table 3.1 Characteristics of Polystyrene

Polystyrene Sample	M_w	M_w/M_n	$[\eta]$ (ml/g) (in Toluene)	M_v
PSF-2000	20.6×10^6	—	2177.9	18.2×10^6
PSF-850	8.42×10^6	1.17	1168.2	8.21×10^6
PSF-550	5.48×10^6	1.15	842.03	5.42×10^6
PSF-380	3.84×10^6	1.04	646.61	3.87×10^6
PS-14A	1.65×10^6	1.19	357.86	1.83×10^6
PSF-128	1.09×10^6	1.08	245.18	1.13×10^6

3.2 Single-Pass Flow System

3.2.1 Apparatus

The laboratory pipe flow apparatus is a pressure driven capillary flow device that was designed to test at various Reynolds numbers using small fluids volumes in a single-pass going through the test section. In this system, the fluid is not exposed to any moving parts (i.e., pumps). Thus the shear degradation to the polymers is kept to a minimum. However, shear degradation can be important for high molecular weight polymers in the strong turbulent field. Therefore, the degradation studies were performed by using multiple passes through the system. The advantage in this type of system is that the magnitude of shear that the polymer solutions have been exposed to can be directly controlled and calculated, unlike the systems that use in-line pumps as the driving force for fluid flow. A schematic of the apparatus is given in Figure 3.2-1.

The fluid reservoir (f) is a 1-liter, high pressure vessel (rated to 1000psi) which is made of stainless steel (316-SS) and fitted with SS tees at the top and bottom. At the top, a 2-way ball-valve (Whitey) (e) is mounted on the vertical branch of the tee to allow for the pressure relief and the filling of the reservoir with solution. The horizontal branch is connected to the pressure delivery system, which is composed of a 2-way ball-valve (Whitey) (d), a fine-flow regulator valve (Grove Loader^{TM}) (c), a gas reservoir (500 ml) (b) which damps out the pressure fluctuations and provides a constant pressure driving force, and a high pressure nitrogen gas supply (a). Off the bottom of the fluid reservoir, one branch of the tee is attached to a pressure gauge (Matheson; 0-60psi) (g), through standard 1/4" (O.D.) SS tubing to be filled with fluid prior to the experiment. The other branch leads to the test section. The tubing between the fluid reservoir and the 2-way ball-valve (Whitey) (h) immediately preceding the capillary (I), is standard 1/2" (O.D.) SS. The capillary is coupled directly into the ball-valve by using a 45^0 Flared reduction

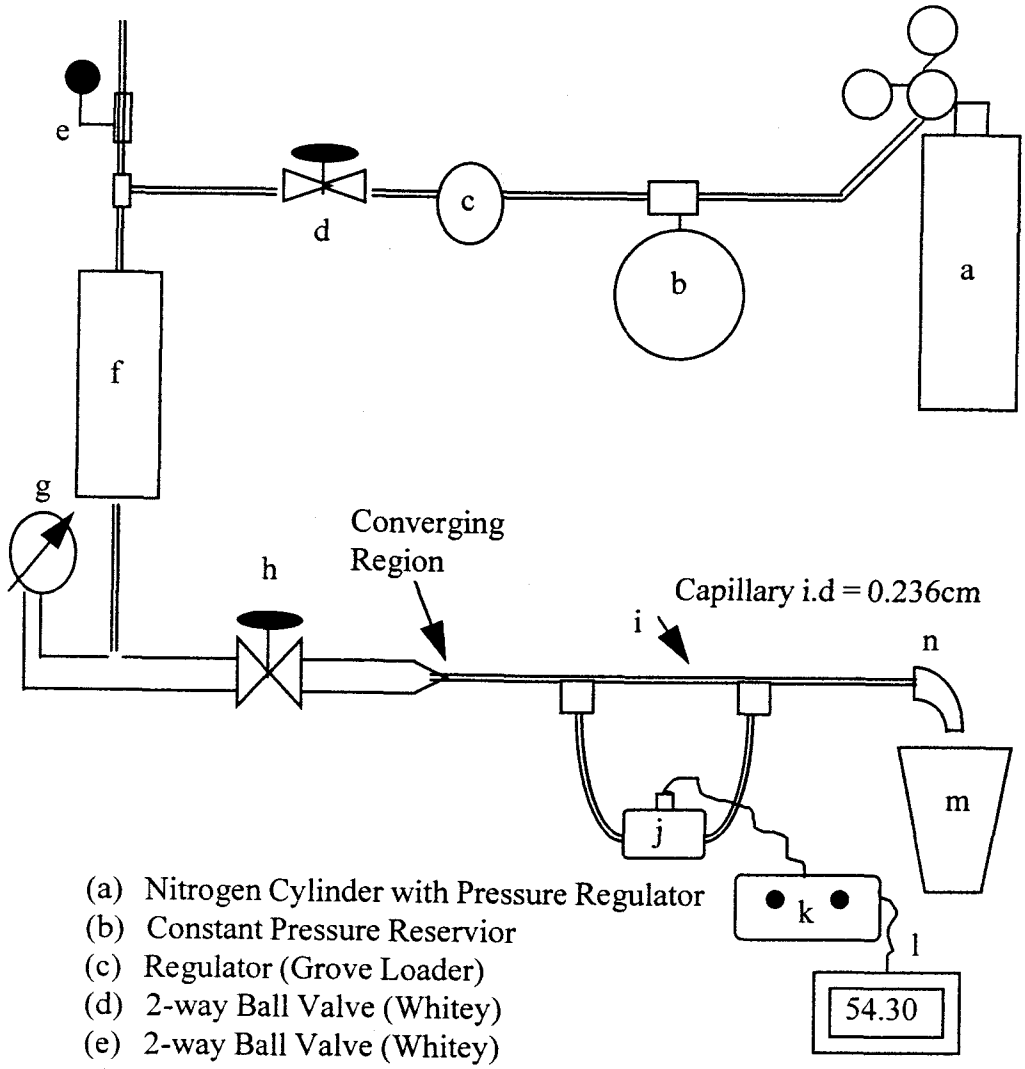

(a) Nitrogen Cylinder with Pressure Regulator
(b) Constant Pressure Reservior
(c) Regulator (Grove Loader)
(d) 2-way Ball Valve (Whitey)
(e) 2-way Ball Valve (Whitey)
(f) Fluid Reservior (1 Liter)
(g) Pressure Gauge (0-60 psig)
(h) 2-way Ball Valve (Whitey)
(i) Stainless Steel Capillary (i.d. = 0.236cm)
(j) Differential Pressure Transducer
(k) Carrier Demodulator
(l) Digital Readout (+/- 0.01psi)
(m) Collection Beaker
(n) Plastic Tube

Figure 3.2-1 Schematic of Laboratory Pipe Flow Apparatus

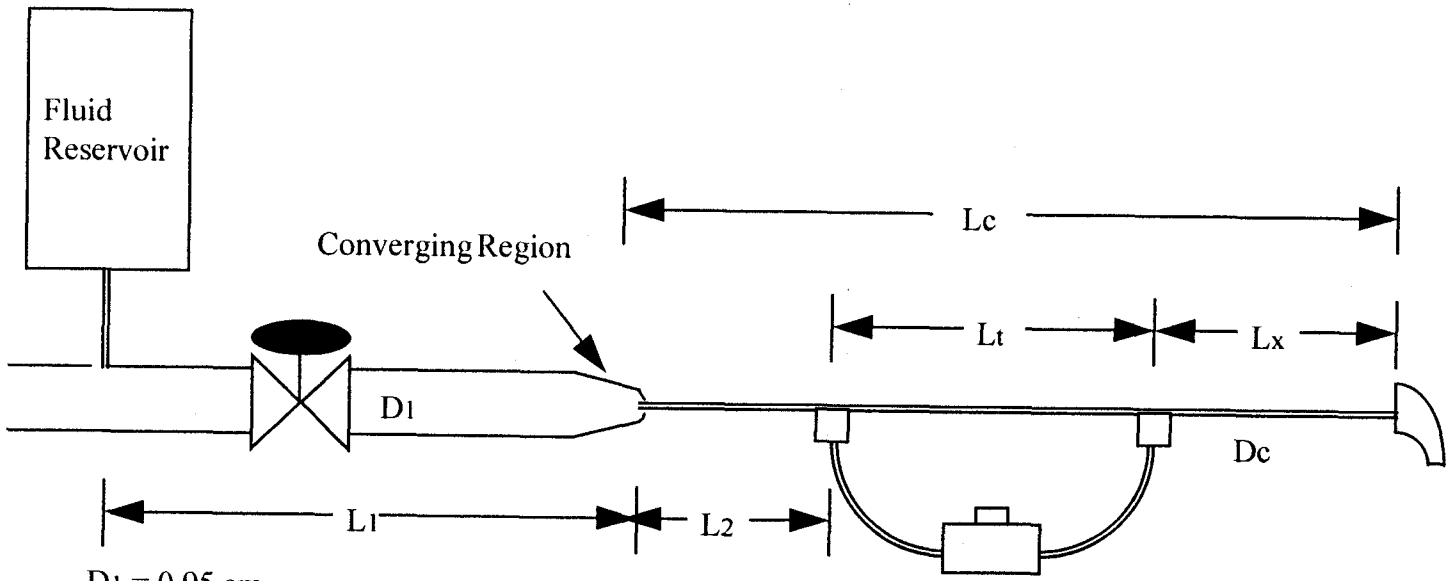

$D_1 = 0.95$ cm
$L_1 = 46.25$ cm
Dc (Capillary Diameter) = 0.236 cm
Lc (Capillary Length)= 62.9 cm
L_2 (Entrance Section Length) = 16 cm
Lt (Test Section Length) = 25.4 cm
Lx (Exit Section Length) = 21.5 cm
Le (Entrance Length) = $L_2/Dc \sim 68$
Contraction Ratio = $D_1/Dc \sim 4$

Figure 3.2-2 Detailed Schematic of the Capillary

fitting which is attached to its end. The capillary (I) is 0.236 cm (i.d.), hydrodynamically smooth SS tubing. The pressure drop is measured by using a variable reluctance differential pressure transducer (Celesco Model DP-15 with a 15psid pressure plate) (j) which is coupled with a carrier demodulator (Validyne Model CD-15) (k) accompanied with digital readout (l). The mass flow rate was measured by collecting the effluent from the capillary in a 1000ml beaker in a time period. The time of each run was measured by using a stop watch.

A detailed schematic of the capillary is given in Figure 3.2-2, including all the geometric dimensions necessary to make the appropriate flow calculations. The section of tubing preceding the capillary is included in this schematic because of the importance of the flow field development to the drag reduction measurements. The length (L_1) has been measured to the center of the tee at the bottom of the fluid reservoir. The distance from the capillary entrance to the first pressure tap is L_2; the distance between the pressure taps is Lt; the distance from the second pressure tap to the capillary exit is Lx; and the total capillary length is Lc. The entrance length is Le = (L_2/Dc) ~ 68. The coupling of the capillary with the rest of the test section is through a 45^0 Flare male fitting coming out of the ball-valve with i.d. = D_1, and a 45^0 Flare female reduction fitting attached to the end of the capillary. This achieves a converging conical section with a 90^0 taper at the entrance to the capillary. The contraction ratio in the converging section is (D_1/Dc) ~ 4.

3.2.2 Procedure

Prior to the actual drag reduction experiment, the calibration of the transducer and several equipment adjustments have to be made. These will be discussed in some

detail and then the procedure for a typical drag reduction experiment will be outlined in this section.

The transducer calibration was conducted as follows. The desired pressure plate was inserted into the Celesco transducer. For most of the experiments the 15 psid pressure plate was used to obtain the correct pressure drops. Each time the pressure plate was removed or the transducer was opened for any reason (e.g., cleaning), recalibration was required. The calibration was done using only N_2 gas so that the system had to be purged of all liquid before starting. There are two 6 inch lines of high pressure tubing leading from the taps on the capillary to the high and low pressure sides of the transducer (this is a differential pressure transducer). The line from the low pressure side of the transducer was removed and plugged, as was the end of the capillary. The pressure gauge (g) was removed and a mercury manometer was attached in its place. This was done because of the increased accuracy available with the manometer. As valves (e) and (h) were opened, the manometer and CD-15 were zeroed. Valve (e) was then closed, valve (d) was remained open, and the system was pressurized by adjusting the regulator valve (c). (Note: The pressure in the gas reservoir (b) was maintained at 110 psig.) The absolute system pressure was read from the manometer and the corresponding transducer reading was taken from the digital readout (l). A plot of the absolute pressure versus the transducer reading was then made and the linear least squares fit of the data was used as the calibration curve for the calculation of pressure drop. Similarly, the calibration was also done on the low pressure side (i.e., pressure plate deflection in the opposite direction), with no significant difference noted. Hence, the high pressure side calibration was used for all calculations.

To ready the apparatus for an experiment, the first step was to fill the fluid reservoir with DIW or toluene and, with valve (h) closed, remove the pressure gauge (g), bleed the line to the gauge under gravity flow until it was clean and free of air bubbles, and replace the gauge. In all cases, the line to the gauge was filled with the solvent which

was used in the drag reduction experiment (i.e., DIW or toluene). The next step was to flush the system by closing valve (e), opening valve (d), pressurizing the fluid reservoir using regulator (c) (to ~30-40 psig as measured on the pressure gauge), and opening valve (h). Once the fluid was in the system, the lines to the pressure transducer could be bled. There are bleed ports on either side of the transducer housing to allow each side to be purged independently. This can be done conveniently by plugging the end of the capillary, pressurizing the system and alternately opening each of the bleed ports until a bubble-free flow of liquid was observed from the port. This indicates that both the lines to the transducer and the small compartment in the transducer housing are filled with fluid.

With all these preparations completed, an experimental run could be made. Before each DR experiment, the pure solvent was run through the system to make sure that the Newtonian turbulent data could be reproduced. This was always taken as the reference point for the calculation of %DR. The solvent was gravity-fed into the fluid reservoir through valve (e), and the system was flushed several times at 30-40 psig. New solvent was added to the fluid reservoir, valve (e) was closed, valve (d) was opened, and the reservoir was pressurized to the desired level using regulator (c). (Note: As was mentioned previously, the pressure in gas reservoir (b) was maintained at ~ 110 psig at all times, and no pressure greater than 155 psig was ever used in these experiments, thus there were no problems with pressure fluctuations in the driving system) When the transducer was properly zeroed, valve (h) was opened. Data acquisition was initiated after ~50-100 ml of fluid had passed through the system and continued until another 200-700 ml had been collected. To note the time, a stop watch was used as was mentioned previously. When steady flow conditions were reached and the appropriate readings could be taken, the run was terminated by closing valve (h). The pressure drop was manually recorded from the digital readout (l) under steady flow conditions during the experiment. At most flow rates the pressure readings were very constant, but when the

flow rate was in the turbulent transition region the pressure reading "bounced" quite a bit, and it made more difficult to get an accurate value. (Note: This "bouncing" in the pressure reading was a very good qualitative indicator of the nature of the transition region and the growing turbulent intensity of the flow.) The system pressure was then relieved by closing valve (d) and opening valve (e). The fluid was either discarded (single-pass experiments) or saved to be retested.

The procedure for conducting a DR experiment with polymer solution was quite similar. The system was always flushed with 200-300 ml of the solution that was to be tested before starting the experiment. The data for the single-pass experiments were obtained by going from low to high flow rates, and the solution was discarded after each pass through the system. Degradation experiments were conducted in two ways. In one case, the solution was run over and over again at the same pressure setting, and the pressure drop data were obtained as a function of the number of passes through the system at that particular flow rate. At the next flow rate the procedure was repeated until all the flow rates had been covered. The data obtained from these experiments were drag reduction as a function of the number of passes through the system at a particular Reynolds number. In the second case, a typical single-pass experiment was performed for all flow rates, after which the solution was passed through the system any number of times (typically 10-20 passes) at the maximum possible flow rate. The single-pass experiment was then repeated with the degraded material. The data obtained in this case were a comparison of drag reduction versus Reynolds number for a new and a degraded material. The main intention of doing the second type of experiment is to examine how a material which is exposed to severe flow conditions behaves over the entire flow region (i.e., both low and high Reynolds numbers). Flow rate and pressure drop were recorded in all experiments, from which Reynolds number and friction factor were calculated. The viscosity term in the Reynolds number was based on the viscosity of solvent.

CHAPTER 4
RESULTS AND DISCUSSION

The experimental results of drag reduction will be discussed in the following sections. As was mentioned in previous chapters, the plots of the f vs Re format and the Prandtl-von Karman format will be used to present the drag reduction data.

The polymer solutions are very dilute in most cases but they are of such high molecular weight so that they may exhibit a non-Newtonian viscosity (shear rate dependence), especially at the very high shear rates encountered in the turbulent flow. Due to the ambiguity in defining a shear rate in the turbulent flow field, the difficulty in obtaining viscosity vs. shear rate data for the polymer solutions, and the questions related to whether the extensional viscosity (which can be several orders of magnitude higher than the shear viscosity) is the "controlling" parameter, it was decided to use the **solvent viscosity to calculate the Reynolds number (Re) in all cases**. In choosing the solvent viscosity for the Re calculation, the value of the onset wall shear rate will always be somewhat higher than the actual value, which means that the calculated value of De will also be larger than the actual value. From the low shear rate viscosity data, it can be estimated that these values could be no more than 10% larger. This approach, although conservative, was deemed to be the most unbiased way to analyze the data.

4.1 Dependence of Onset on Molecular Weight

Figure 4.1-1 shows the experimental results for three different molecular weight polystyrene samples, PSF-380, PSF-550, and PSF-850, at approximately the same concentration of 100ppm. The point where the data intersect the solvent line (Blasius Expression) defines the onset condition which includes the values of friction factor, fluid velocity and wall shear rate ($\dot{\gamma}_w^*$) at onset (see Equation 2.3-8). As can be seen in Figure 4.1-1, it is evident that the wall shear rate at onset decreases with increasing molecular weight.

Based on the discussion in Sections 2.4 and 2.5, the drag reduction phenomenon is proposed to occur as the polymer chains in the solution begin to be extended. The studies done by Miles and Keller (1980) in a biaxial elongational flow experiment, found that the extensional rate needed for polystyrene molecules of higher molecular weight to be fully extended is smaller than that for polystyrene molecules of lower molecular weight. As the higher molecular weight polystyrene molecules begin to be stretched out at lower shear rates, the activated molecules subsequently result in an effective elongational viscosity increase in the flow. The increased elongational viscosity will damp the turbulent eddies and accomplish the drag reduction. The reason that the higher molecular weight polystyrene molecules require less shear rate to be extended in the process of extension may due to that the cross area of an individual polystyrene molecule is proportional to its molecular weight. Since the molecule of higher molecular weight apparently has a larger cross area of exposure to the flow, it can be expected that the

Figure 4.1-1 Onset as a Function of MW

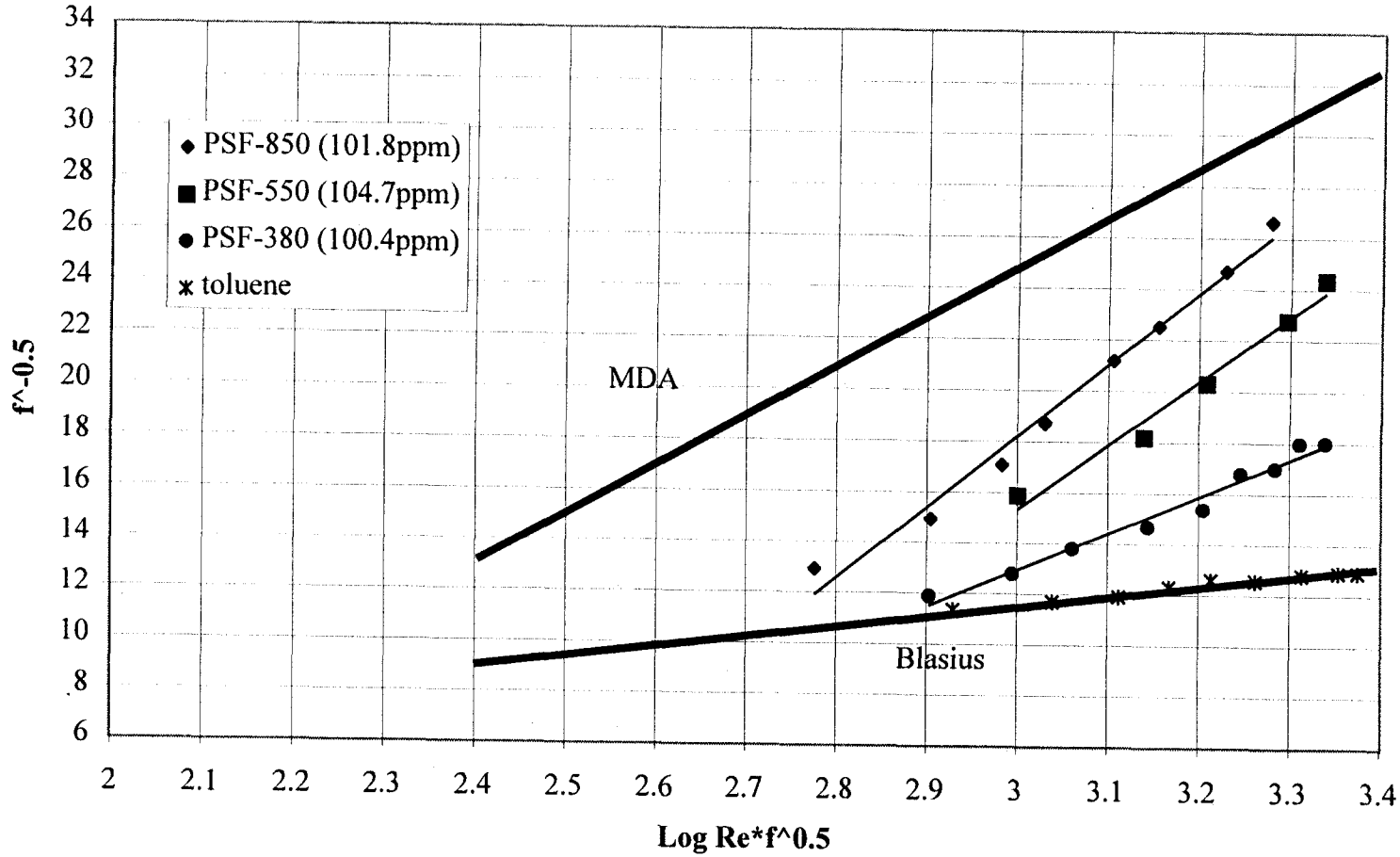

molecule can be extended at lower shear rates. Thus the drag reduction occurs at lower shear rates.

According to Time Scale theories, the onset occurs when $De = \dot{\gamma}_w^* \tau_m \sim 1.0$ (see Equation 2.4-2) and the polymer terminal relaxation time calculated from Zimm theory is proportional to molecular weight. Assuming that the Time Scale theories are correct, the wall shear rate at the onset point for higher molecular weight polystyrene is expected to be smaller to keep $De \sim 1.0$. This is consistent with the results presented in Figure 4.1-1.

4.2 Dependence of Onset on Concentration

Since it appears that molecular weight determines the onset of turbulent drag reduction, it is important to understand if polymer concentration would effect onset. Time Scale theories would predict a very weak dependence based solely on the effect of concentration on polymer relaxation time. The Zimm theory used to calculate τ_m does not have an explicit concentration dependence, but rather uses the value of intrinsic viscosity (in finite dilution) in its calculation. This could be modified to include a concentration dependence if that was warranted.

The concentration dependence of onset for each polystyrene sample was determined by taking data at a minimum of three different concentrations. The results for PSF-850 ($MW=8.42\times10^6$) are shown in Figure 4.2-1. The results indicated that the wall shear rate at the onset point systematically decreases with an increase in concentration, although the differences are small.

In contrast, the experimental results for the onset point shown in Figure 4.2-2 for PSF-380 ($MW=3.84\times10^6$) appear to be independent of the concentration. These results are in agreement with the previous experiments conducted by Berman (1977), in which an onset independence of concentration for a random coiling polymer in a good solvent was observed. However, the dependence of onset on concentration was also observed for the same polymer in a part of Berman's experiments. Berman related the differences in onset behavior to molecular weight distribution effects.

Based on the results of present and previous studies, it is difficult to arrive at a definitive conclusion for the dependence of onset on concentration. Since the polymer terminal relaxation time calculated from Zimm theory is actually a weak function of concentration, following Time Scale theories, the change in concentration should cause a shift in the onset point.

Although the flow rate dependence of drag reduction was proposed in previous studies to be related to the "top-part" of the molecular weight distribution, the number of activated molecules in the "top-part" of the distribution increases with an increasing concentration and consequently the drag reduction level at each flow rate above the onset point will increase. Therefore, when the concentration increases, these molecules of very high molecular weight may reach a concentration at which they can lower the onset shear rate.

However, since the polystyrene samples used in this study are narrow distribution polymers, the results can help to conclude that the onset appears to have a relatively small dependence on concentration.

Figure 4.2-1 Drag Reduction Results for PSF-850 (MW=8420000)

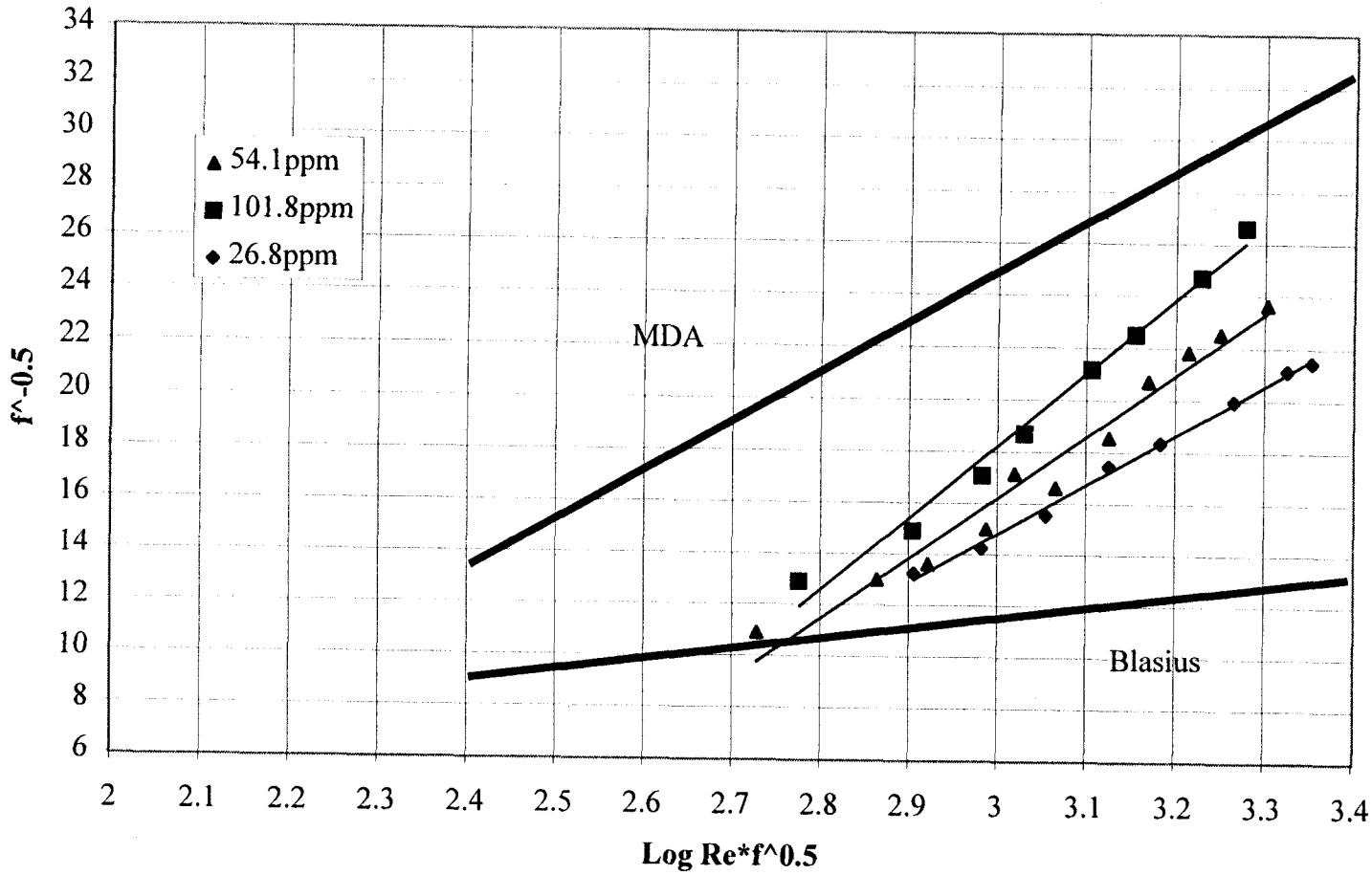

Figure 4.2-2 Drag Reduction Results for PSF-380 (MW=3840000)

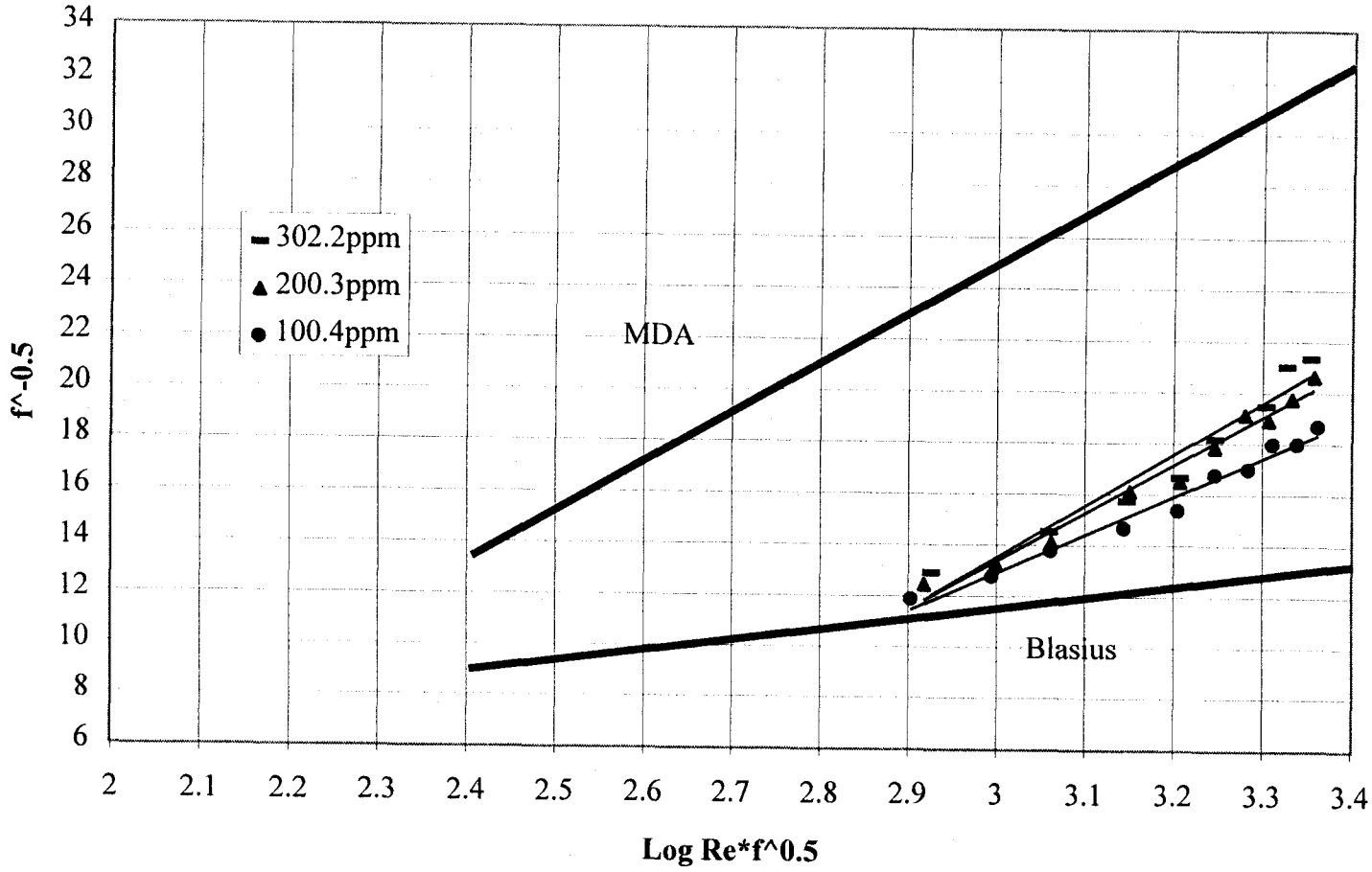

4.3 Examination of Time Scale Theories on Onset

Since the onset phenomenon, which is important both from a theoretical and an application point of view, has been intensively studied, a lot of previous works proved that Time Scale theories are the most successful theories to predict the onset point. It can be noted again that the onset point proposed by Time Scale theories occurs when De = $(\dot{\gamma}_w^*)(\tau_m) \sim 1.0$. However, the experiments done by Zakin and Hunston (1980) on polystyrene samples have shown that the data of Deborah number at the onset point have a value about one order of magnitude larger than that predicted by Time Scale theories (De = 10 ~ 30).

To examine Time Scale theories, the experimental results of four polystyrene samples of different molecular weight were used. Figure 4.3-1 and Figure 4.3-2 show the results for PSF-550 ($MW=5.48\times10^6$) and PS-14A ($MW=1.65\times10^6$), respectively. Including the results shown in Figure 4.2-1 and 4.2-2, the wall shear rate at the onset point, where the data intersect the solvent line, can be calculated (Equations 2.3-7 and 2.3-8). By using Equation 2.4-2, the polymer terminal relaxation time for each polystyrene sample can be determined and subsequently the Deborah number (De). Values of Deborah numbers at the onset point for polystyrene samples at various concentrations are shown in Table 4.3.

As can be seen in Table 4.3, the Deborah number remains approximately constant with relatively small variations over a wide range of concentrations and molecular weights. A weak concentration dependence on Deborah number at the onset point is

Figure 4.3-1 Drag Reduction Results for PSF-550 (MW=5480000)

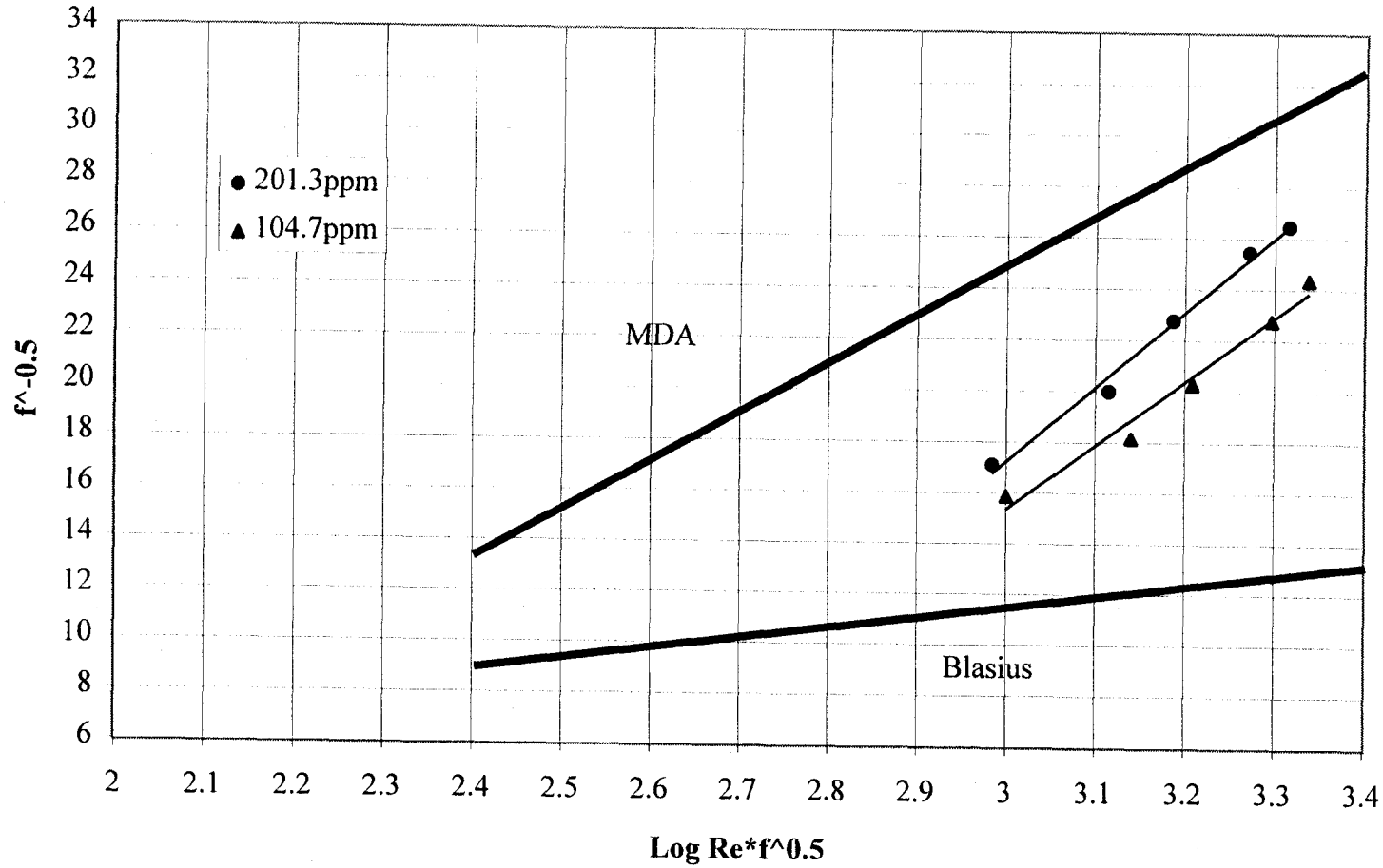

Figure 4.3-2 Drag Reduction Results for PS-14A (MW=1650000)

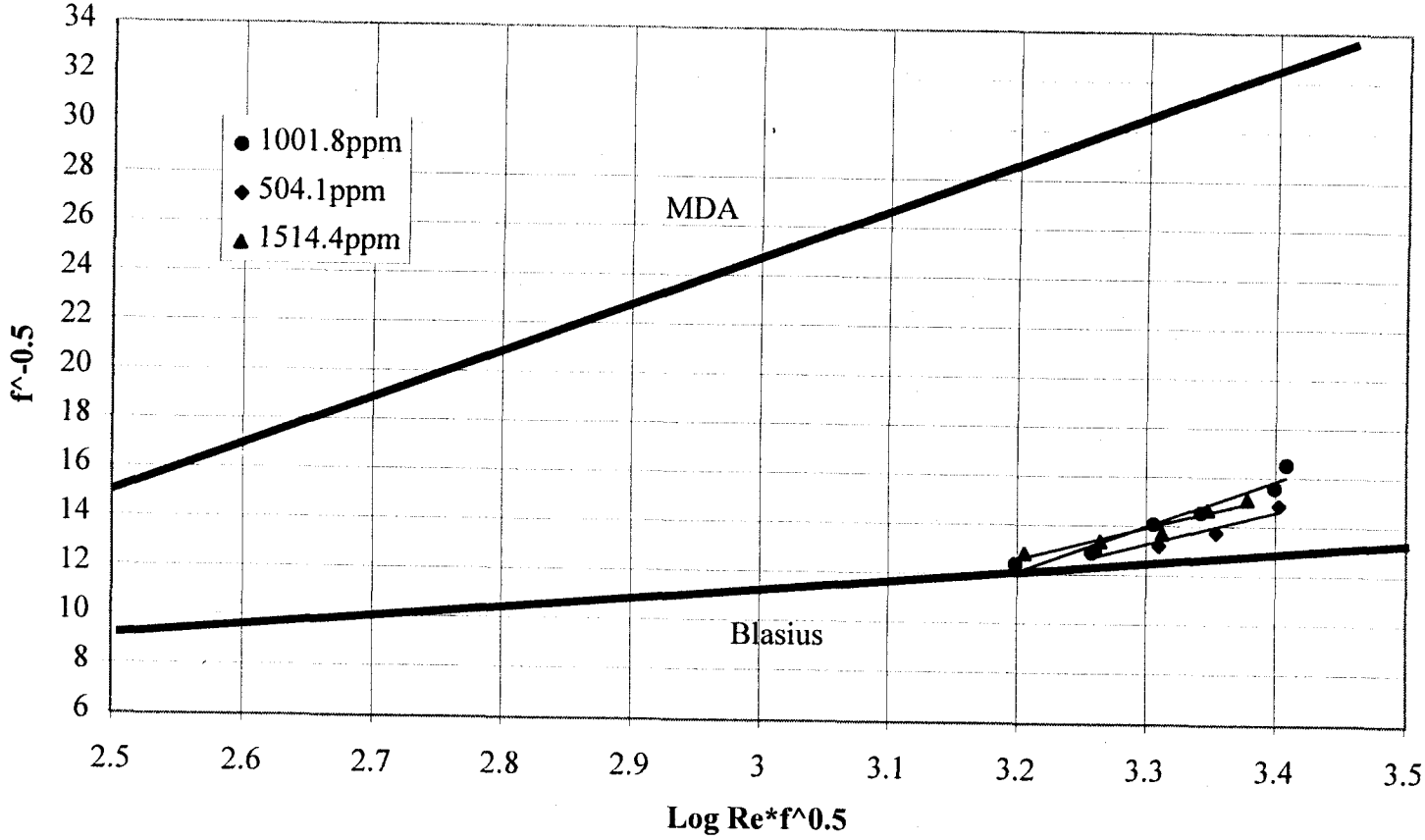

again observed as Deborah number decreases with increasing concentration. However, the value of De $\approx 8 \sim 20$ is about one order of magnitude larger than the value predicted by Time Scale theories, and is consistent with the results of Hunston and Zakin.

According to Time Scale theories, the molecule will begin to be extended when it is exposed to a strong flow field. The extended molecule will then cause an increase in the local viscosity which leads to damping of turbulent, and subsequently drag reduction.

It has been suggested by previous workers, and experimentally verified in the exquisite experiments of Miles et. al. (1980) that an extensional ("strong") flow is much more effective than a shear ("weak") flow (which has vorticity) in "activating" molecules through the coil-to-stretch transition. That is necessary for large molecular extensions and subsequently large extensional viscosities (10 ~ 1000 times greater than shear viscosities for high molecular weight polymers).

Consider that in a highly turbulent flow, the encounter-rotating turbulent eddies would provide a strong local extensional flow, which could "activating" molecules and lead to large, local extensional viscosities. This raises the question of weather the average wall shear rate is the appropriate deformation rate to be used in calculating De. It suggests that an "extension rate" associated with the encounter-rotating turbulent eddies might be more appropriate.

Assuming that a polymer molecule in the bulk flow is an individual particle, Batchelor (1980) derived the mean rate of extension along the vortex lines (E_w) in the turbulent motion where the particle is immersed. The results of Batchelor's calculations are that $E_w \cong 0.1 \dot{\gamma}_w$.

Table 4.3 Deborah Number at Onset

Polystyrene	Concentration (ppm)	f_{onset}	Re_{onset}	τ_m (sec)	$\dot{\gamma}_w^*$	De_{wall}	De_{eddy} ($=\tau_m \times E_w$)
PSF-850 MW=8.42×10^6	26.8	0.0091	5679.9	1.01×10^{-3}	17981	18.2	1.82
	54.1	0.0094	4988.8	1.01×10^{-3}	14320	14.5	1.45
	101.8	0.0096	4585.9	1.01×10^{-3}	12289	12.4	1.24
PSF-550 MW=5.48×10^6	104.7	0.0087	6798.8	4.7×10^{-4}	24570	11.6	1.16
	201.3	0.0089	6207.9	4.7×10^{-4}	20950	9.9	0.99
PSF-380 MW=3.84×10^6	100.4	0.0081	9048.3	2.5×10^{-4}	40518	10.1	1.01
	200.3	0.0081	9048.3	2.5×10^{-4}	40518	10.1	1.01
	302.2	0.0081	9048.3	2.5×10^{-4}	40518	10.1	1.01
PS-14A MW=1.65×10^6	504.1	0.0066	20527	6×10^{-5}	169918	10.2	1.02
	1001.8	0.0067	19329	6×10^{-5}	152940	9.2	0.92
	1514.4	0.0068	18217	6×10^{-5}	137874	8.3	0.83

If the mean extensional rate along the vortex lines was used to calculate Deborah number instead of the mean wall shear rate, the values of Deborah number in Table 4.3 were reduced to one tenth of original values. Surprisingly, the resultant values are much closer to that predicted by Time Scale theories with De = 0.83 ~ 1.82. Apparently, the mean extensional rate along the vortex lines in turbulent flow is a more appropriate quantity to be used in Time Scale theories to predict the onset point.

4.4 Dependence of Drag Reduction on Molecular Weight

Figure 4.4-1 compares the drag reduction effectiveness (%DR) of three polystyrene samples, PSF-850, PSF-550, and PSF-380 at various Reynolds numbers. All polystyrene solutions were tested at a concentration of about 100ppm. The results in Figure 4.4-1 have shown that the %DR increases with an increase in molecular weight. The results imply that the %DR is a strong function of molecular weight (MW). Since the dimension of a higher molecular weight molecule is larger than that of a lower molecular weight molecule, it can be expected that the extended molecule of higher molecular weight can be more efficient to damp the turbulent eddies due to its larger dimension and consequently bring out the higher drag reduction effectiveness.

It is shown in Figure 4.4-1 that the drag reduction effectiveness of the three polystyrene samples initially increases rapidly with increasing an Reynolds number and approaches a maximum value at high Reynolds number region.

Figure 4.4-1 Drag Reduction as a Function of Molecular Weight

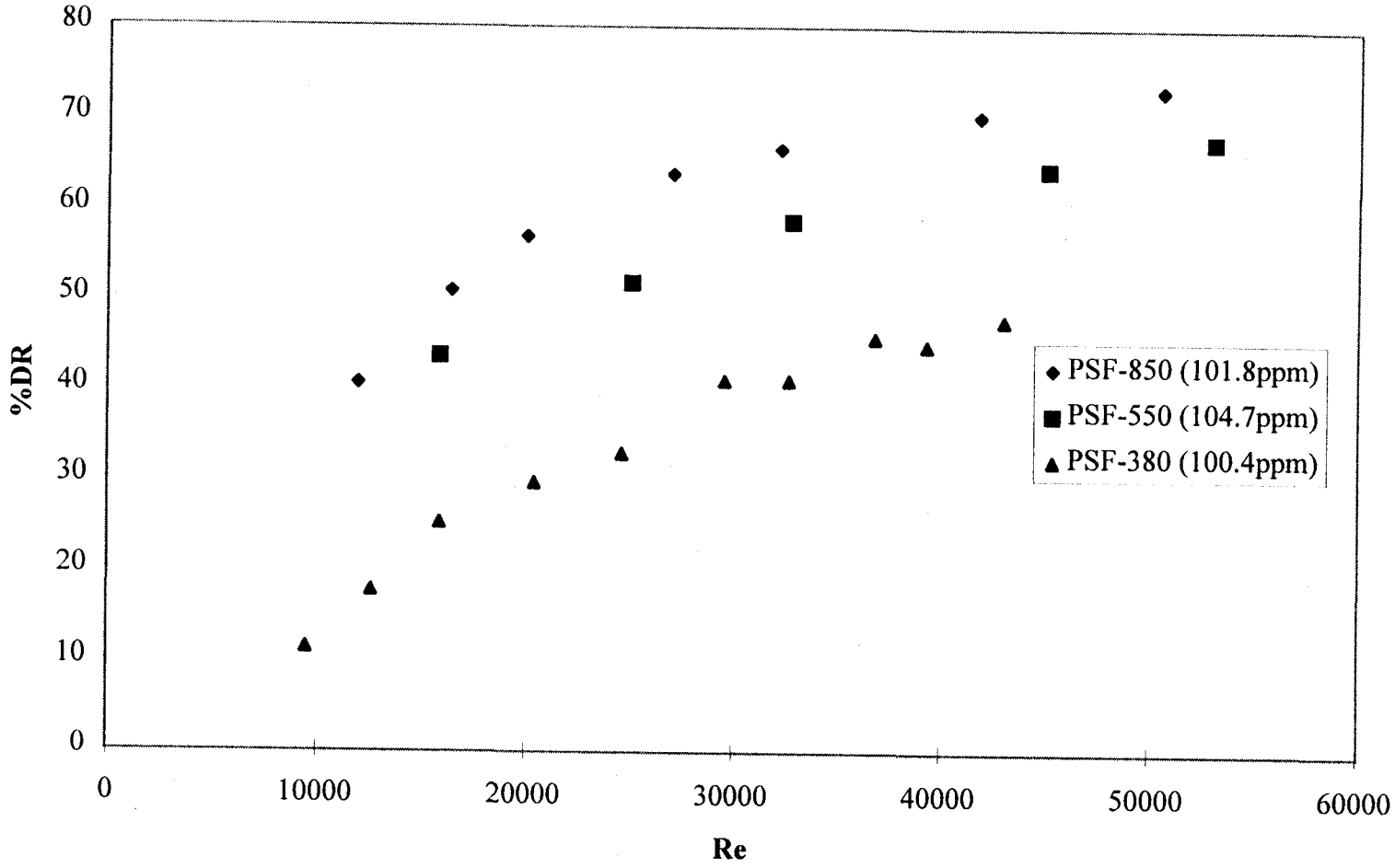

4.5 Dependence of Drag Reduction on Concentration

Since drag reduction is caused by the sum of the contributions from individual polymer molecules, an increase in concentration of polymer solutions can increase the amount of drag reduction. The dependence of drag reduction for PSF-850 ($MW=8.42\times10^6$) as a function of polymer concentration is shown in Figure 4.5-1. The data clearly indicate that the drag reduction effectiveness increases with increasing concentrations. The results shown in Figure 4.2-2 and 4.3-1 also indicate that the increasing polymer concentration can cause larger drag reduction effectiveness as the slopes of the data, which represent the drag reduction efficiency, increase with higher concentrations. As a result, concentration is obviously playing another key factor in the drag reduction effectiveness.

Figure 4.5-2 shows the results of concentration dependence of the drag reduction effectiveness for PS-14A ($MW=1.65\times10^6$). In this case, the drag reduction effectiveness of polystyrene solution at C = 1512.4ppm has a larger value compared to the solution at C = 1001.8ppm for low Re, but it shows a smaller value at high Re. The results are quite different from the results obtained from any other polystyrene sample.

Once polymer molecules begin to be extended in a flow field, they may have a greater possibility of intermolecular contact as the number of molecules increases. As a result, the interactions between extended polymer molecules will take place when the number of molecules in the solution exceeds an optimum value and thus will result in a decrease in the drag reduction effectiveness. Moreover, compare to the solution in which

Figure 4.5-1 Drag Reduction as a Function of Concentration for PSF-850 (MW=8420000)

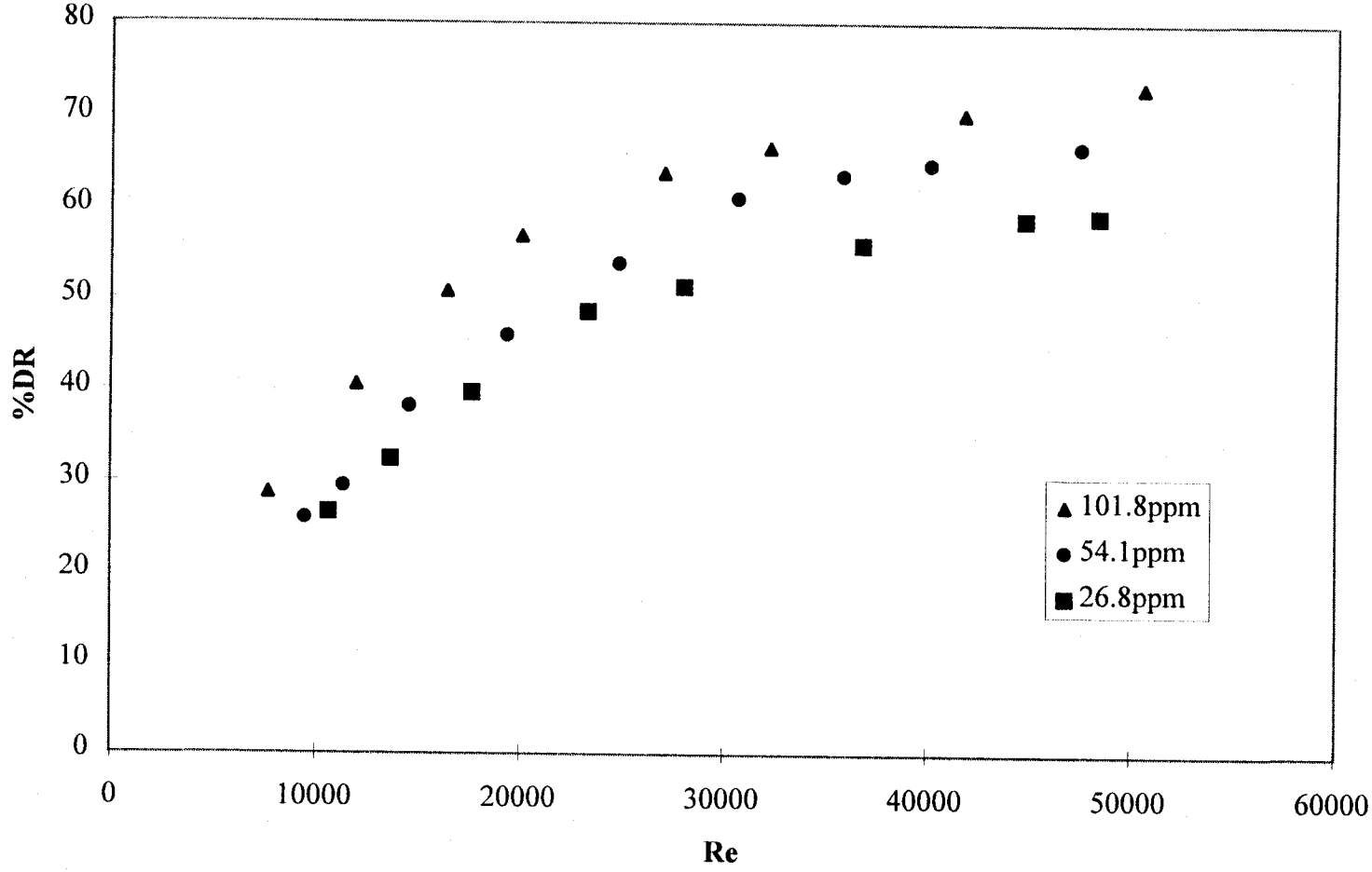

Figure 4.5-2 Drag Reduction as a Function of Concentration for PS-14A (MW=1650000)

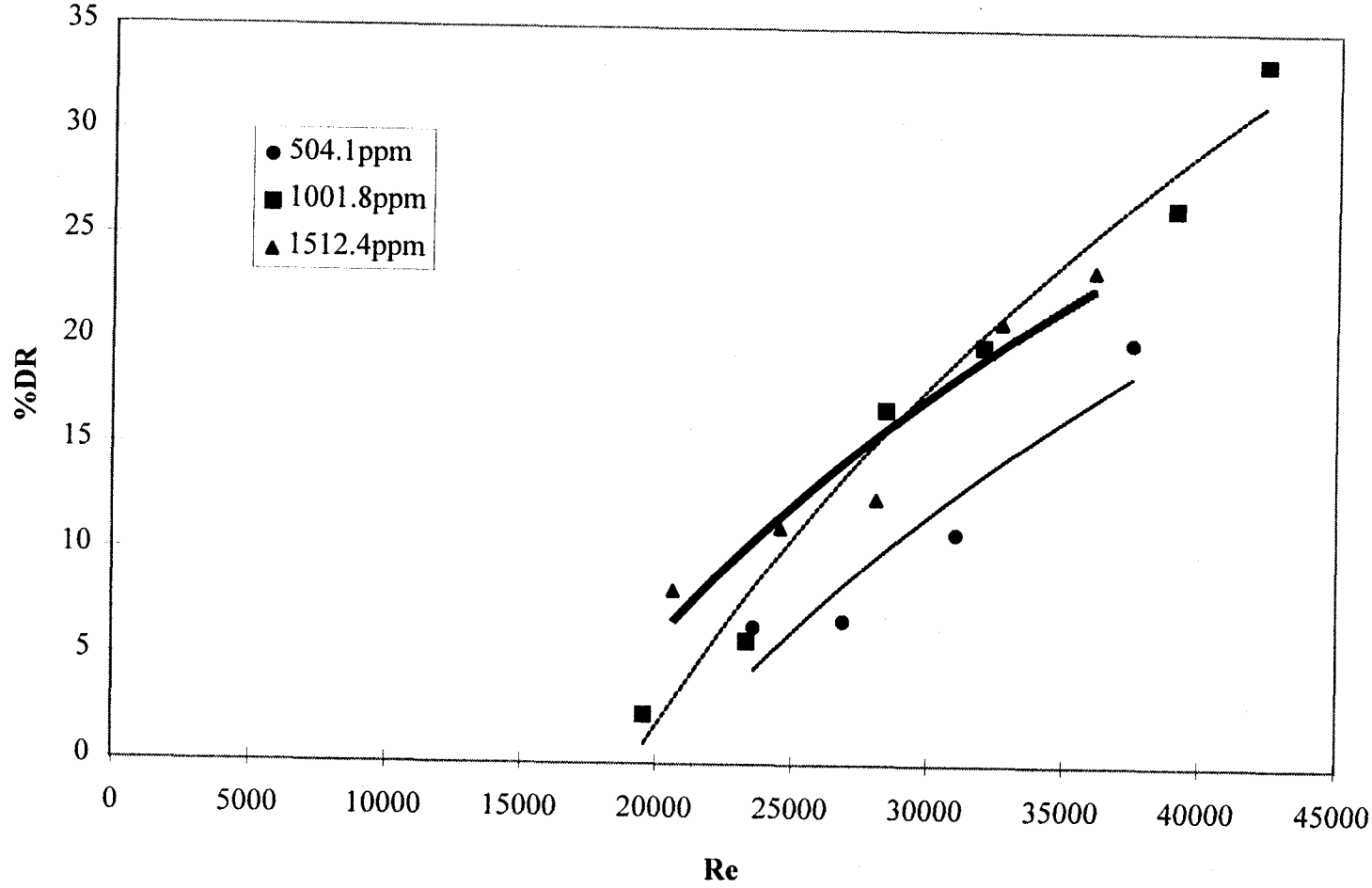

a smaller number of molecules are present, the space for molecules to be freely extended is less in the solution of a relatively larger number of molecules and consequently the stretching process of molecules will be hindered. Thus, the drag reducing efficiency of polymer solutions will decrease as the concentration exceeds an optimum value. Furthermore, as the concentration is increased, however, an increase in the solution viscosity is also obtained. This increase in the solution viscosity brings out an increase in drag. As a result, the drag reduction effectiveness reaches a maximum value, and decreases as the increased solution viscosity becomes a dominant factor in the drag of the solution. In the case of the polystyrene (PS-14A) solution at C = 1512.4ppm, the viscosity of the solution is approximately 1.8 times larger than that of the solvent. Thus, the less %DR of the solution compared to the lower concentration solution may be due to the great increase in viscosity.

4.6 Examination of Ryskin's "Yo-Yo" Theory of Drag Reduction

Although the "Yo-Yo" theory presented by Ryskin had it's shortcomings, the appealing aspect of the theory, and the main reason that attracted so much attention when it was first introduced, was that it was one of the first theories to attempt to quantitatively predict the drag reducing effectiveness of a polymer solution. All of the Length, Time, and Energy theories previously focused on the prediction of the onset of drag reduction, not the effectiveness once onset was achieved. Ryskin's theory did not predict onset. Instead, it focused on how the polymer molecule responded after it was "activated" and

attempted to predict it's effectiveness as a drag reducer. This attempt at a quantitative prediction of %DR was new and appealing.

Ryskin's theory did not account for polydispersity (molecular weight distribution) in polymer samples. In fact, it assumed that the drag reducing polymer had a single terminal relaxation time. Unfortunately, in his original work Ryskin chose to use drag reduction data for a water soluble polymer with a very broad molecular weight distribution, and possibly even a very high molecular weight tail to test his theory. This led to a great amount of skepticism for researches in this field, many of whom were already working with model polymer systems (such as narrow distribution polystyrenes) and were well aware of the difficulties in interpreting data for polydisperse, water soluble polymers.

Surprisingly, even though there was much publicity (both pro and con) surrounding Ryskin's theory in 1987, it does not appear that up to this time it has been properly tested with a well-characterized series of model polymers. A proper test of the Ryskin's theory was attempted in this work with the model polystyrene samples. The molecular parameters for the four polystyrene samples used are given in Table 3.1 and the drag reduction data are presented in Figures 4.2-1, 4.2-2, 4.3-1 and 4.3-2. The experimental data are plotted in Prandtl-von Karman coordinate so that the slope increment can be easily calculated. For each set of drag reduction data, the slope increment was used to "back-calculated" the values of α (see Equation 2.5-8) and κ (see Equation 2.5-5) using the concentration and intrinsic viscosity. The results are shown in Table 4.6.

In Ryskin's paper, he assumed that $\kappa = 0.3$ as constant and that $\alpha = 0.18$ should be the value for polymers with methylene, oxyethylene, and siloxane backbones. As can be seen in Table 4.6, neither of these assumptions is consistent with the experimental data of this thesis, in which κ varies from 0.27 to 0.55 and α varies from 0.15 to 0.33.

The values of the slope-increment (drag reducing effectiveness) calculated from Ryskin's theory with $\kappa = 0.3$ and $\alpha = 0.18$ are also given in Table 4.6 for the various polystyrene samples. Once again, this points out rather dramatically the failure of the Ryskin's theory since the predicted slope-increments are $2 \sim 3$ times smaller than the experimental values. Therefore, the Ryskin's theory grossly underestimates the drag reducing effectiveness of the model polystyrene materials.

In addition to the obvious deficiencies in Ryskin's theory pointed out by the present studies, recent numerical work by Hinch (1994) found that the "Yo-Yo" type of uncoiling for the center of molecules proposed by Ryskin is not what was observed in three-dimensional simulations of molecules in an extensional flow field. Instead, there appears to be a gradual buildup of many "fully stretched" chain segments, with no "coiled ends" observed. Thus, it may be that the fundamental premise of the Ryskin's theory, the mechanism of molecular deformation is also in error.

Table 4.6 Comparison of Ryskin's Theory Prediction and Experimental Data for Slope-Increment

		Experimental Data			Ryskin's Theory Prediction		
Polystyrene	**concentration (ppm)**	κ	δ (slope-increment)	α	κ	α	δ (slope-increment)
PSF-850	26.8	0.27	15.17	0.33	0.3	0.18	4.99
	54.1	0.31	19.72	0.29	0.3	0.18	8.11
	101.8	0.36	24.13	0.25	0.3	0.18	12.18
PSF-550	104.7	0.34	21.16	0.31	0.3	0.18	7.10
	201.3	0.39	25.23	0.26	0.3	0.18	10.90
PSF-380	100.4	0.31	10.99	0.29	0.3	0.18	4.15
	200.3	0.37	14.86	0.25	0.3	0.18	6.80
	302.2	0.41	16.19	0.22	0.3	0.18	8.96
PS-14A	504.1	0.40	9.27	0.25	0.3	0.18	3.92
	1001.8	0.48	14.75	0.24	0.3	0.18	6.44
	1514.4	0.55	9.21	0.15	0.3	0.18	8.51

4.7 Effects of Molecular Weight Distribution on Onset and Drag Reduction

As has been discussed previously, molecular weight distribution (polydispersity) has always been an issue in drag reduction studies, particularly with broad molecular weight distribution (MWD) water soluble polymers that have dominated the drag reduction literature for the past 50 years. There have been very few drag reduction studies using well-characterized, model polymers, and even fewer that have addressed the MWD effect in a systematic and controlled fashion. An issue related to MWD is the long standing question of which molecules in the MWD are providing all the effects. This is especially important when attempting to declare the concentration dependence of the drag reduction. A part of this question is if the presence of a "high molecular weight tail" dominates the drag reduction behavior.

It has long been speculated, particularly in the most popular and effective water soluble polymer systems such as the anionic polyacrylamides, that a very high MW component (maybe $> 10^7$) was principally responsible for the effectiveness of these polymers at very low concentrations of 5 ~ 10ppm. This had never been tested, and that is what motivated the present studies of mixing two well-characterized polymers of very different MW to obtain a bimodal molecular weight distribution, and in particular, to study a bimodal distribution in which one of the polymers is of extremely high molecular weight and present in very small amounts (high molecular weight tail effect).

First, two binary mixtures were tested in the studies. Each mixture was prepared by mixing two polystyrene samples, PSF-850 and PS-14A, at specified concentrations.

The concentrations of PS-14A ($MW=1.65\times10^6$) were kept approximately at 500ppm in the two mixtures. The concentrations of PSF-850 ($MW=8.42\times10^6$) changed from 26ppm to 50.6ppm in the two mixtures. The results are shown in Figure 4.7-1, along with the individual drag reduction data for each of the pure components.

Two things are apparent from Figure 4.7-1. First, the drag reduction effectiveness achieved by the mixture is always greater than the individual drag reduction effectiveness achieved by either component. Second, increasing the higher molecular weight component in the mixture increases the overall drag reduction. The results clearly point out that the drag reduction is largely dominated by the molecules with the highest molecular weight. This means that the top of the molecular weight distribution in polydisperse samples causes the occurrence of the drag reduction.

Since the top of the molecular weight distribution was found to greatly dominate the overall drag reduction, the results shown in Figure 4.7-1 indicate that the onset point is dictated by the largest molecules in the molecular weight distribution. However, a shift in the onset point for the mixtures, comparing to the solutions which contain only the higher molecular weight component, was observed in Figure 4.7-1.

To explain the phenomena, the discussion on the onset point in previous sections has to be recalled. Since the onset is predicted to occur when $De \sim 1.0$, any change in the polymer terminal relaxation time will result in a shift in the onset point.

When the other lower molecular weight polystyrene sample is dissolved in the solvent, the viscosity of the solvent which is referred to the solution without the further addition of higher molecular weight polystyrene sample, can be expected to rise to an

Figure 4.7-1 Drag Reduction for Mixtures containing PSF-850 and PS-14A

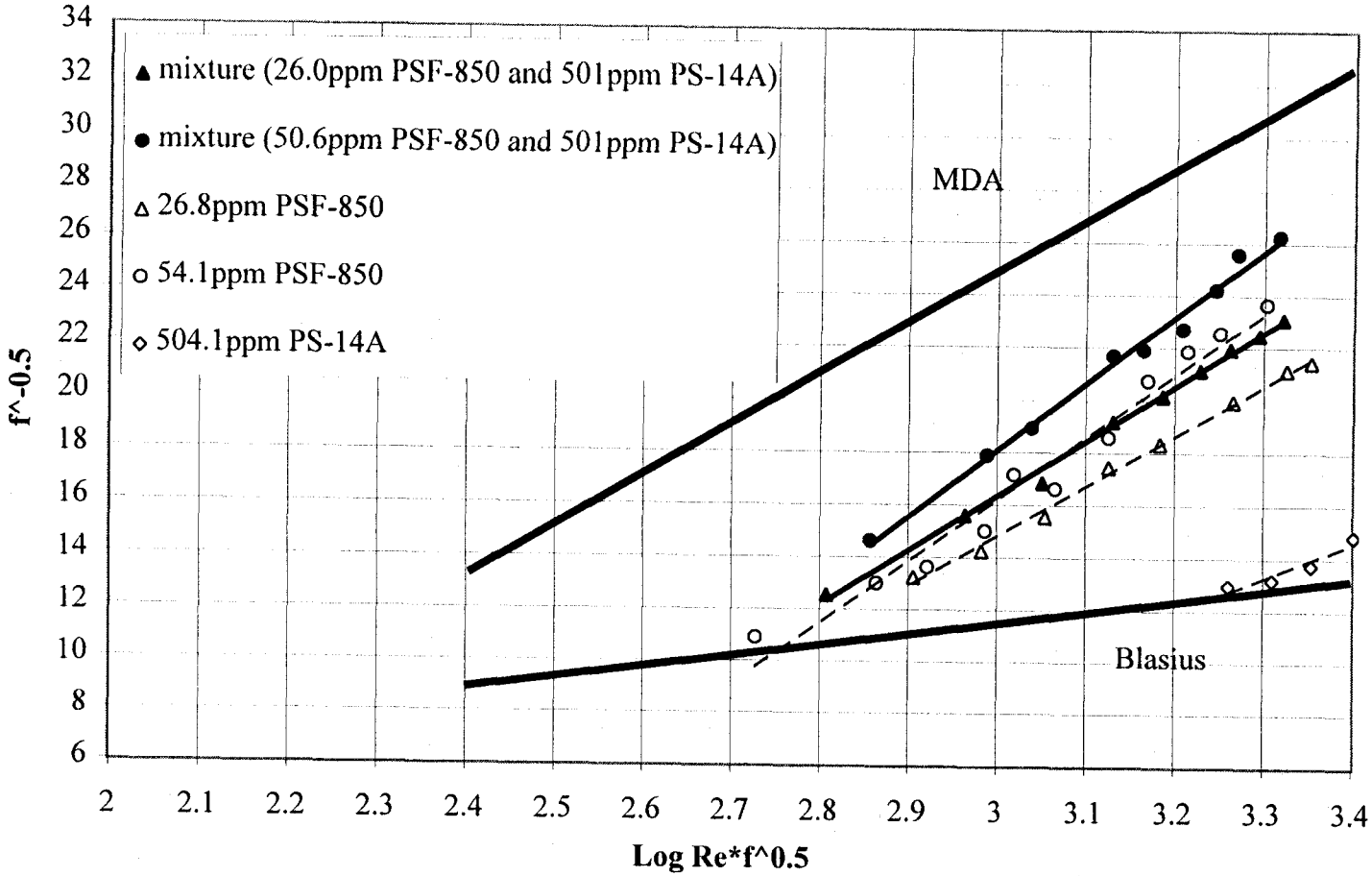

extent due to the presence of the lower molecular weight polystyrene sample. Since the polymer terminal relaxation time is proportional to the solvent viscosity (see Equation 2.4-2), the increased solvent viscosity will lead to a larger value of the relaxation time for the higher molecular weight polystyrene component. As a consequence, a lower onset shear rate is observed for the mixtures. The effect can be easily observed from the results shown in Figure 4.7-1.

The onset data for the mixtures are listed in Table 4.7, including the data for higher molecular weight polystyrene component. The results show that the Deborah numbers at the onset for the higher molecular weight component in the mixtures are surprisingly close to the values obtained from the solutions that contain only the higher molecular weight component at the indicated concentrations. This is a strong indication that both the drag reduction and the onset point depend on the largest molecules in the molecular weight distribution.

Table 4.7 Onset Data for Mixtures

Polystyrene	**Solvent Viscosity (poise)**	f_{onset}	Re_{onset}	τ_m **(PSF-850) (sec)**	$\dot{\gamma}^{*}_{w}$	**De** $(=\tau_m \times E_w)$
Mixture (26.0ppm PSF-850 & 501ppm PS-14A)	0.0071	0.0098	4222.8	1.21×10^{-3}	15558	1.88
PSF-850 (26.8ppm)	0.0059	0.0091	5679.9	1.01×10^{-3}	17981	1.82
Mixture (50.6ppm PSF-850 & 501ppm PS-14A)	0.0071	0.0101	3743.0	1.21×10^{-3}	12540	1.51
PSF-850 (54.1ppm)	0.0059	0.0094	4988.8	1.01×10^{-3}	14320	1.45

Figure 4.7-2 Drag Reduction for Mixtures containing PSF-2000 and PSF-380

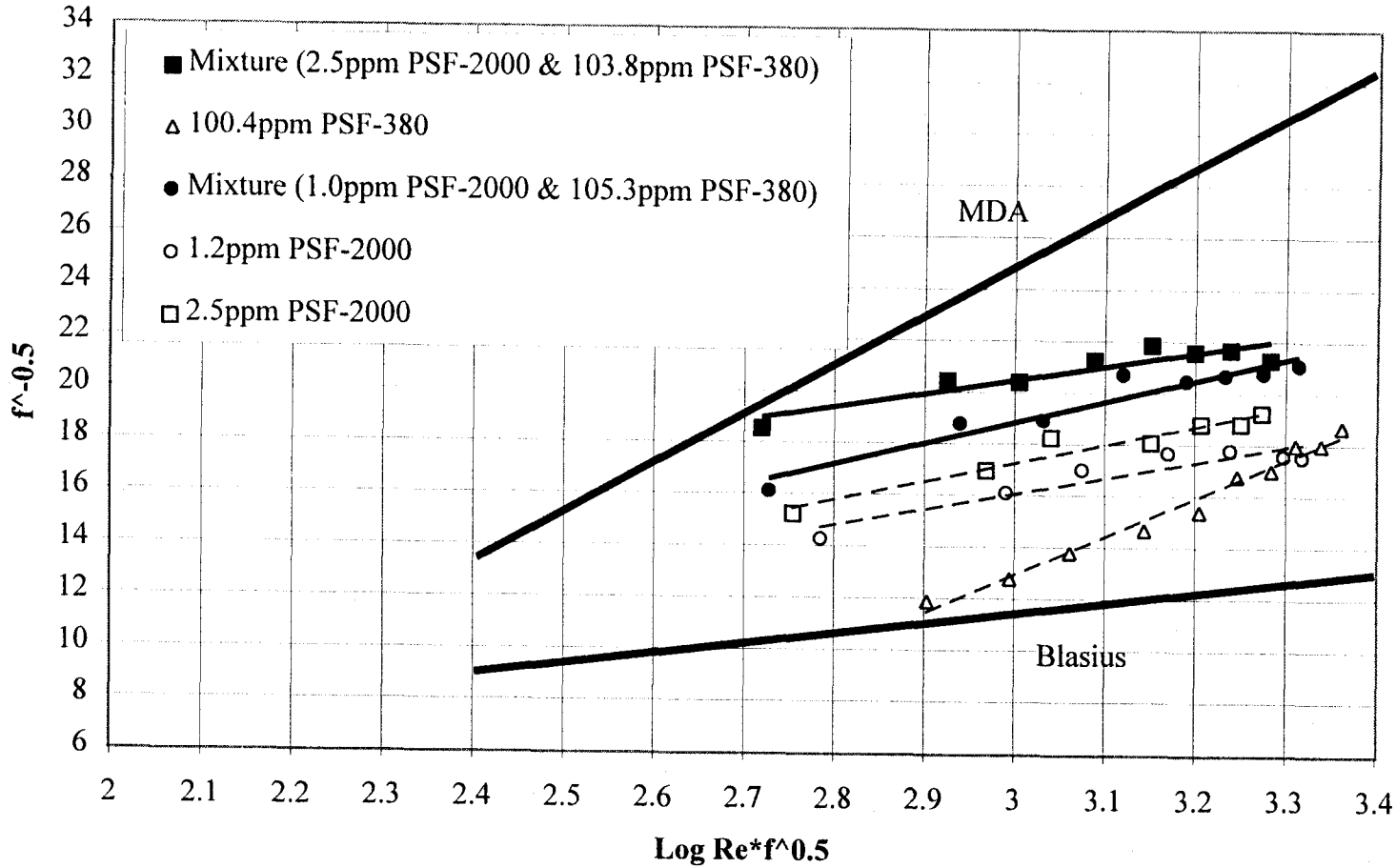

Figure 4.7-3 Drag Reduction for Mixtures containing PSF-2000 and PSF-128

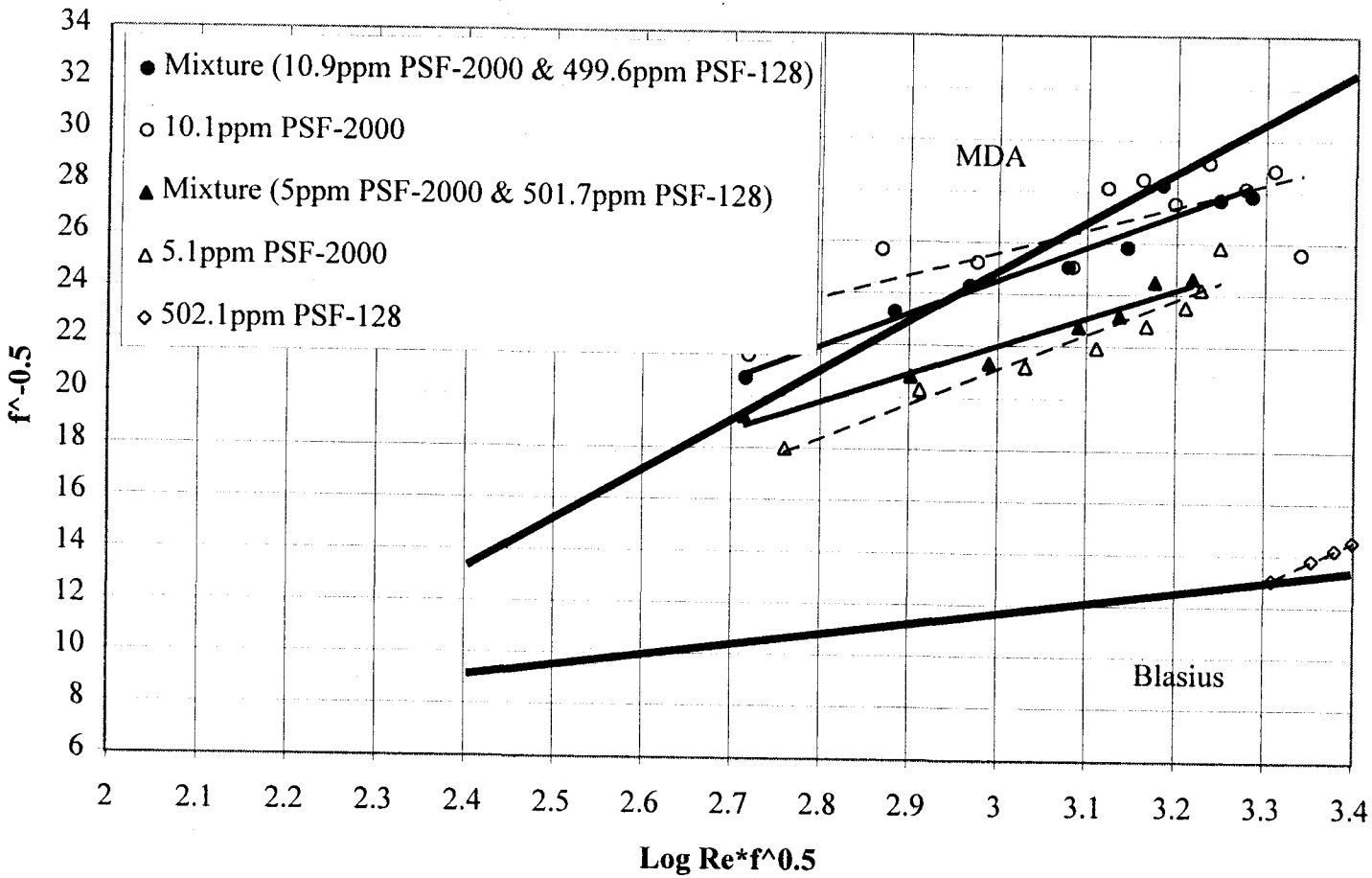

Figure 4.7-2 and Figure 4.7-3 show the drag reduction results for two binary mixture systems combining PSF-2000 with PSF-380 and PSF-128, respectively. In the first mixture system, the concentrations of PSF-380 were held approximately at 100ppm and the concentrations of PSF-2000 were changed from 2.5ppm to 1.0ppm in the two mixtures. The results clearly demonstrate the dominance on both the onset and the drag reduction of the higher molecular weight component (PSF-2000), even with the presence of only 1.0ppm in the mixtures. This is the clear indication in the drag reduction literature of the absolute importance (dominance) of the high molecular weight tail on the drag reducing effectiveness of polymer solutions. It also substantiates the data on water soluble polymer systems that show substantial drag reduction at extremely low concentrations ($C \cong 1.0$ppm). It clearly demonstrates that for a substantial amount of %DR to occur at very low concentrations, there has to be a very high molecular weight component ($MW > 10^7$) to the polymer.

4.8 Degradation Studies

Although polystyrene was found to be a good drag reducing polymer, one of the major problems with this material is that polystyrene can be shear degraded under high shear conditions of the pipe flow apparatus, and subsequently lose its drag reducing capability. This is a problem especially in the multiple pass systems, where the polymer solution may make hundreds of passes around a flow loop. Thus, the use of polystyrene as a drag reducer has always been in single pass systems.

To study the degradation of polystyrene samples, the experiments were carried out by running the same solution repeatedly for up to 8 runs through the single-pass flow system at a set driving pressure (i.e., approximately the same Re or wall shear rate, $\dot{\gamma}_w$), and measuring the ΔP on each pass to determine the friction factor. The degraded solution after the degradation tests was collected for relative viscosity measurements.

Tables 4.8-1 and 4.8-2 show the changes in the relative viscosities of polystyrene solutions before and after the degradation tests conducted at the specific Re. The results indicate that the relative viscosities of the fresh polymer solutions are systematically greater than that of the degraded solutions. Based on the discussion in Section 3.1.2, the relative viscosity is a parameter which characterizes molecular weight of polymers and is directly proportional to molecular weight. It is evident that polystyrene samples in the solutions were indeed degraded in the degradation tests.

Table 4.8-1 Capillary Relative Viscosity Measurements of Drag Reduction Solutions

Polystyrene	Concentration (ppm)	$[\eta]$	C^* (ppm)	C/C^*	η_{rel} (fresh solution)	η_{rel} (degraded solution) 10th pass
PS-14A	504.1	357.86	3030.0	0.17	1.195	1.182 (Re ≅ 40000)
	1514.4	357.86	3030.0	0.50	1.773	1.652 (Re ≅ 40000)
PSF-380	100.4	646.61	1557.6	0.06	1.067	1.060 (Re ≅ 46000)
	302.2	646.61	1557.6	0.19	1.212	1.205 (Re ≅ 46000)
PSF-550	201.3	842.03	1176.9	0.17	1.155	1.133 (Re ≅ 55000)
PSF-850	26.8	1168.2	839.0	0.03	1.035	1.017 (Re ≅ 47000)
	54.1	1168.2	839.0	0.06	1.055	1.049 (Re ≅ 47000)

Table 4.8-2 Shear Degradation Study - Viscosity Effect

		η_{rel} (degraded solution)		
Polystyrene	Re	1st pass	5th pass	10th pass
PSF-550 201.3ppm η_{rel} (fresh solution) = 1.155	≅ 16000	1.152	1.150	1.149
	≅ 47000	1.136		
	≅ 55000	1.135	1.133	1.133
PSF-2000 10.1ppm η_{rel} (fresh solution) = 1.017	≅ 56000	1.003		

4.8.1 Effect of Molecular Weight on Degradation

Two polystyrene samples of different molecular weight were run through the system at approximately the same concentration to study the effect of molecular weight on degradation. The degradation tests were conducted at $\dot{\gamma}_w \cong 3.2\times10^5\ s^{-1}$ for both polystyrene samples. The results for these experiments using PSF-550 and PSF-380 are given in Figure 4.8-1. As can be seen in Figure 4.8-1, PSF-550 ($MW=5.48\times10^6$) shows a greater increase in friction factor values than the sample of $MW=3.84\times10^6$ after each successive run in the degradation tests. The increase in friction factor indicates a lower drag reduction and subsequently a decrease in molecular weight. Thus it is evident that the higher molecular weight polystyrene is more susceptible to the shear degradation. Since the higher molecular weight polystyrene is more effective in reducing the drag, the increase in friction factor is therefore larger once the polystyrene is degraded.

Figure 4.8-1 Effect of Molecular Weight on Degradation

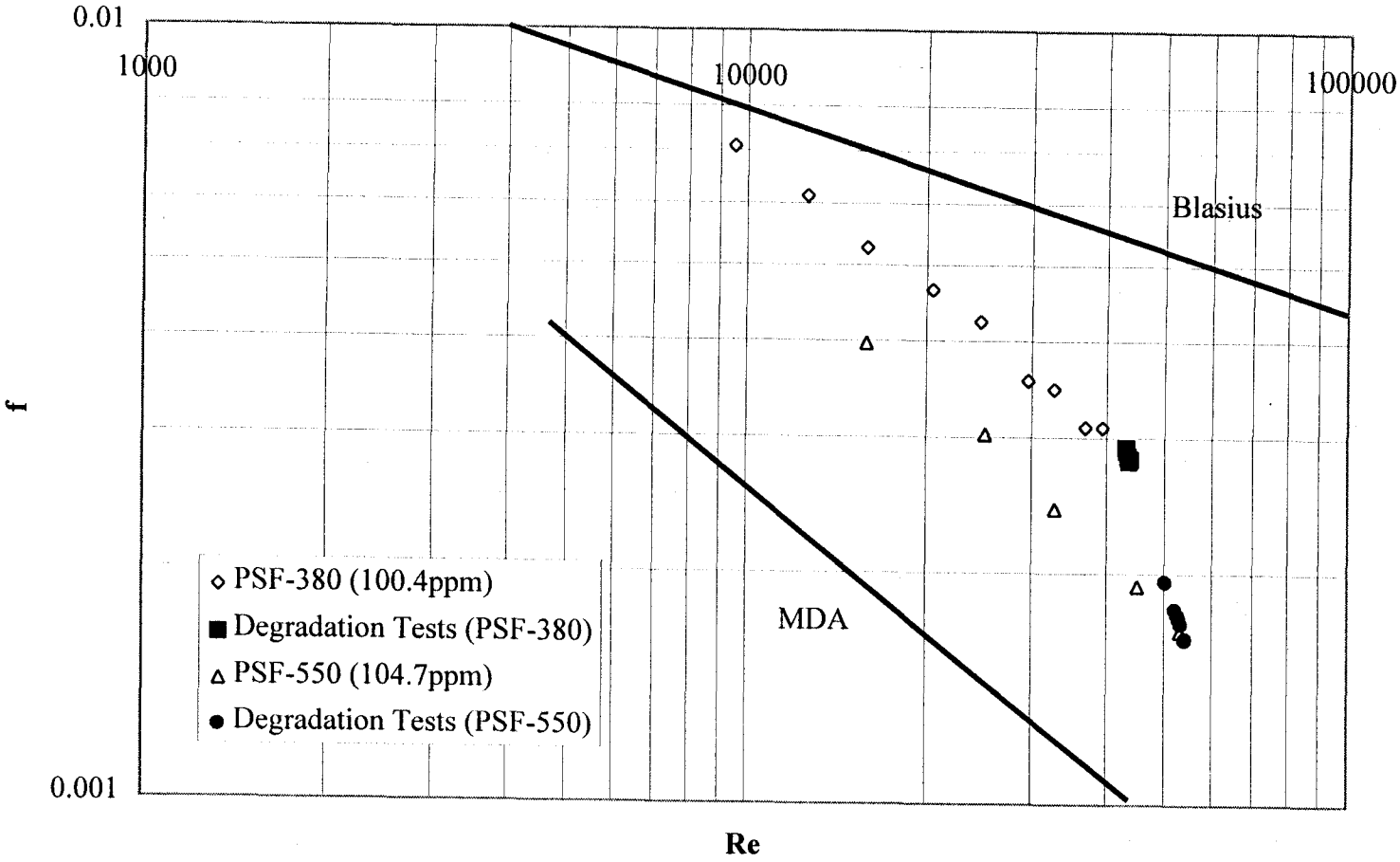

Figure 4.8-2 Effect of Concentration on Degradation for PSF-850 (MW=8420000)

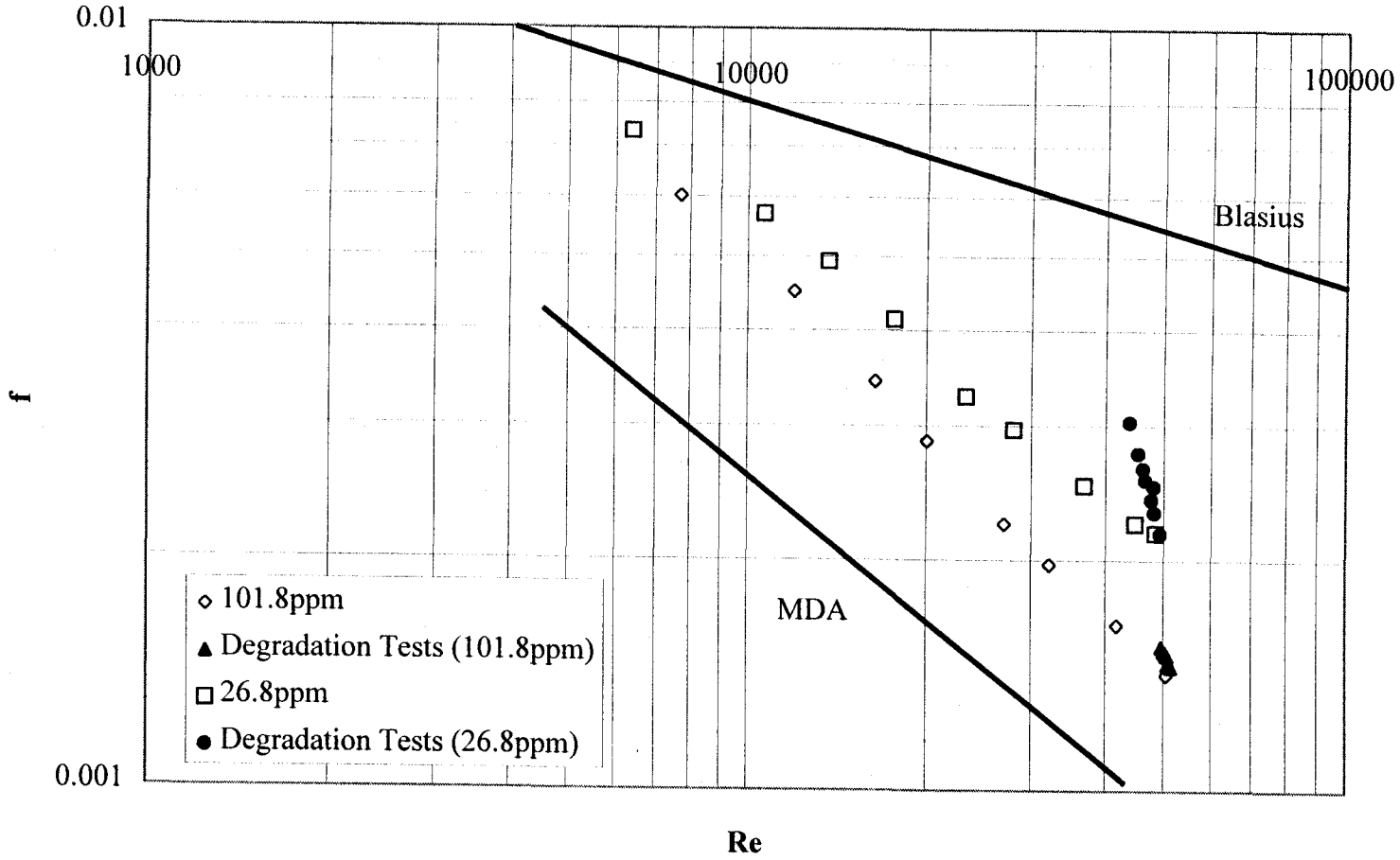

4.8.2 Effect of Concentration on Degradation

Figure 4.8-2 compares the degradation of PSF-850 ($MW=8.42\times10^6$) at two different concentrations of 26.8ppm and 101.8ppm, respectively. The degradation tests were carried out at $Re \cong 50000$. The results show that there is a smaller increase in friction factor for the higher concentration polystyrene solution in the degradation tests. However, it does not imply that the polymer molecules in the higher concentration solution are more resistant to the shear degradation, nor do they remain undegraded after several runs. Since the higher concentration polystyrene solution contains more polymer molecules that help to achieve drag reduction, the results only indicate that there are sufficient undegraded molecules in the higher concentration solution and those can help to maintain a certain level of drag reduction. In other words, polymer molecules are gradually degraded in high shear conditions.

CHAPTER 5
CONCLUSIONS AND RECOMMENDATIONS

On the basis of the present study, the following conclusions can be made:

- Narrow molecular weight distribution, high molecular weight polystyrenes are effective drag reducers.
- A polystyrene of MW > 10^6 is able to achieve substantial drag reduction.
- The onset point for turbulent drag reduction occurs at lower shear rate as the molecular weight of the polymer is increased.
- The dependence of onset on concentration is relatively small, but measurable.
- The mean extensional rate along the vortex lines (E_w) is more appropriately used than the wall shear rate (γ_w) in Time Scale theories to predict the onset point. When this value is used, it is found that the onset point can be predicted to occur at De $\cong$ 0.8 ~ 2.0 for a wide range of molecular weight and concentrations.
- Increasing molecular weight of polymers or increasing concentration of polymer solutions causes an increase in the magnitude of drag reduction (%DR).
- When examined using the experimental drag reduction data for model polystyrenes, Ryskin's "Yo-Yo" theory was found to be deficient in accurately predicting the drag reduction.

- In bimodal mixtures of well-characterized model polystyrene materials, the highest molecular weight component in the mixture systems dominates both the onset and the drag reduction. This is the first conclusive evidence that the high molecular weight tail of the distribution dominates the drag reduction phenomena - onset point and %DR.
- Although higher molecular weight polystyrene can accomplish better drag reduction, it is more readily degraded in high shear conditions.

A detailed study on the mechanism of drag reduction is recommended. The study can also be extended to determine the effects of different variables such as molecular weight, concentration, molecular weight distribution, type of solvent, temperature, and dimensions of the testing pipe on the drag reduction.

BIBLIOGRAPHY

Batchelor, G. K., "Mass Transfer from Small Particles Suspended in Turbulent Fluid", *J. Fluid Mech.*, **98**, 3, 609 (1980)

Berman, N. S., "Flow Time Scales and Drag Reduction", *The Physics of Fluids*, **20**, 10, Pt. II (1977)

Berman, N. S., "Drag Reduction by Polymers", *Ann. Rev. Fluid Mech.*, **10**, 47 (1978)

Bewersdorff, H. W., and N. S. Berman, "The Influence of Flow-Induced Non-Newtonian Fluid Properties on Turbulent Drag Reduction", *Rheol. Acta*, **27**, 130 (1988)

Bewersdorff, H. W., and Albert Gyr, Drag Reduction of Turbulent Flows by Additives, Kluwer Academic. (1995)

Bird, R. B., O. Hassager, and R. C. Armstrong, Dynamics of Polymer Liquids, Vol 1, Fluid Mechanics, John Wiley & Sons, Inc. (1977)

Bird, R. B., O. Hassager, R. C. Armstrong, and C. F. Curtis, Dynamics of Polymer Liquids, Vol 2, Kinetic Theory, John Wiley & Sons, Inc. (1977)

Choi, H. J., and M. S. Jhon, "Polymer-Induced Turbulent Drag Reduction", *Ind. Eng. Chem. Res.*, **35**, 9, 2993 (1996)

Davies, J. T., Turbulence Phenomena, an Introduction to the Eddy Transfer of Momentum, Mass, and Heat, Particularly at Interfaces, Academic Press (1972)

Durst, F., R. Haas, and W. Inerthal, "Laminar and Turbulent Flows of Dilute Polymer Solutions: A Physical Model", *Rheol. Acta.*, **21**, 572 (1982)

Elata, C., J. Lehrer, and A. Kahanovitz, *Isreal J. Techn.*, **4**, 87 (1966)

Fabula, A. G., J. L. Lumley, and W. D. Taylor, in Modern Developments in Mechanics of Continua, Academic Press, New York (1966)

Hershey, H. C., and J. L. Jakin, *Chem. Eng. Sci.*, **22**, 1947 (1967)

Hinch, E. J., "Uncoiling a Polymer Molecule in a Strong Extensional Flow", *J. Non-Newtonian Fluid Mech.*, **54**, 209 (1994)

Hoyt, J. W., "Algal Cultures: Ability to Reduce Fluid Friction in Flow", *Science*, **149**, 1509 (1965)

Hoyt, J. W., "Drag Reduction Effectiveness of Polymer Solutions in the Turbulent-Flow Rheometer: A Catalo", *JPS: Polym. Let.*, **9**, 851 (1971)

Hoyt, J. W., "The Effect of additives on Fluid Friction", *Trans. ASME, J. Basic Engineering*, **94**, 258 (1972)

Hoyt, J. W., "Drag Reduction in Polysaccharide Solutions", *Trends in Biotechnology*, **3**, 17 (1985)

Hunston, D. L., "Effects of Molecular Weight Distribution in Drag Reduction and Shear Degradation", *J. Polym. Sci., Ed. Polymer Chemistry*, **14**, 713 (1976)

Hunston, D. L., and J. L. Zakin, "Effects of molecular Parameters on the Flow Rate Dependence of Drag Reduction and Similar Phenomena", in Viscous Flow Drag Reduction, G. R. Hough, Ed., 72, 373 (1980)

Hunston, D. L., and J. L. Zakin, "Flow-Assisted Degradation in Dilute Polystyrene Solutions", *PE & S*, **20**, 517 (1980)

Kenis, P. R., "Drag Reduction by Bacterial Metabolites", *Nature*, **217**, 940 (1968)

Kenis, P. R., "Turbulent Flow Friction Reduction Effectiveness and Hydrodynamic Degradation of Polysaccharides and Synthetic Polymers", *JAPS*, **15**, 607 (1971)

Kohn, Michael C., "Energy Storage in Drag Reduction Polymer Solutions", *J. Polym. Sci: Pol. Phys. Ed.*, **II**, 2339 (1973)

Kohn, Michael C., "Criteria for the Onset of Drag Reduction", *AICHE J.*, **20**, 185 (1974)

Lumley, J. L., "Drag Reduction in Turbulent Flow by Polymer Additives", *J. Polym. Sci.: Macro. Rev.*, **7**, 263 (1973)

Lumley, J. L., "Drag Reduction in Two Phase and Polymer Flows", *Phys. Fluids*, **20**, (10), Pt. II, S64 (1977)

Metzner, A. B., "Polymer Solution and Fiber Suspension Rheology and their Relationship to Turbulent Drag Reduction", *Phys. Fluids*, **20** (10), Pt. II, S145 (1977)

Miles, M. J., D. P. Pope, C. J. Farrell, and A. Keller, "Conformational Relaxation Time in Polymer Solutions by Elongational Flow Experiments: 1. Determination of Extensional Relaxation Time and its Molecular Weight Dependence, *Polymer*, **21**, 1292 (1980)

Miles, M. J., and A. Keller, "Conformational Relaxation Time in Polymer Solutions by Elongational Flow Experiments: 2. Preliminaries of Further Developments: Chain Retraction; Identification of Molecular Weight Fractions in a Mixture", *Polymer*, **21**, 1295 (1980)

Moussa, T., C. Tiu, and T. Sridhar, "Effect of Solvent on Polymer Degradation in Turbulent Flow", *J. Non-Newtonian Fluid Mech.*, **48**, 261 (1993)

Moussa, T., and C. Tiu, "Factors Affecting Polymer Degradation in Turbulent Pipe Flow", *Chem. Engng. Sci.*, **49**, 10, 1681 (1993)

Mysels, K. J., "Early Experience with Viscous Drag Reduction", in CEP Symposium Series, Drag Reduction, J. G. Savins and P. S. Virk, Eds., No. 111, Vol. **67**, 45 (1971)

Nadolink, R. H., "Friction Reduction in Dilute Polystyrene Solutions", Ph.D. Dissertation, UC. San Diego. (1987)

Nakamura, K., S. Odajima, K. Kizawa, and T. Nakagawa, "Drag-Reducing Effect in Solutions of Very High Molecular Weight Polystyrene by the Rolling Ball Method", *Polymer J.*, **20**, 2, 169 (1988)

Oliver, D. R., and S. I. Bakhtiyarov, "Drag Reduction in Exceptionally Dilute Polymer Solutions", *J. Non-Newtonian Fluid Mech.*, **12**, 113 (1983)

Rabin, Y., F. S. Henyey, and R. K. Pathria, in Polymer Flow Interaction, American Institute of Physics Press (1985)

Rochefort, S., "Xanthan Gum: Rheology and Drag Reduction Studies", Ph.D. Dissertation, UC. San Diego, La Jolla, CA (1986)

Ryskin, G., "Turbulent Drag Reduction by Polymers: A Quantitative Theory", *Phys. Rev. Letters*, **59**, 18, 2059 (1987)

Sellin, R. H. J., and M. Ollis, "Polymer Drag Reduction in Large Pipes and Sewers: Results of Recent Field Trials", *JOR*, **24**, 667 (1980)

Sellin, R. H. J., J. W. Hoyt, and O. Scrivener, "The Effect Of Drag Reducing Additives on Fluid Flows and their Industrial Applications. Part 1: Basic Aspects", *J. Hydraulic Research*, **20**, 29 (1982)

Sellin, R. H. J., J. W. Hoyt, J. Pollert, and O. Scrivener, "The Effect of Drag Reducing Additives on Fluid Flows and their Industrial Application. Part 2: Present Applications and Future Proposals", *J. Hydraulic Research*, **20**, 235 (1982)

Straudinger, H., *Kollod Z.*, Vol. **51**, 71 (1930)

Toms, B. A., in Proc. 1st Intl Congress on Rheology, Sec. II, 135, Amsterdam (1949)

Toms, B. A., "On the Early Experiments on Drag Reduction by Polymers", *Phys. Fluids*, **20**, (10), Pt. II, S3 (1977)

Virk, P. S., E. W. Merrill, H. S. Mickley, K. A. Smith, in Modern Developments in the Mechanics of Continua", Academic Press (1966)

Virk, P. S., E. W. Merrill, H. S. Mickley, K. A. Smith, and E. L. Mollo-Christensen, "The Toms Phenomena in Dilute Polymer Solution Flow", *JFM*, **30**, 305 (1967)

Virk, P. S., and E. W. Merrill, "The Onset of Dilute Polymer Solution Phenomena", in Viscous Drag Reduction, C. S. Wells, Ed., Plenum Press, 107 (1969)

Virk, P. S., H. S. Mickley, and K. A. Smith, "The Ultimate Asymptote and Mean Flow Structure in Toms' Phenomena", *ASME J. Appl. Mech.*, **37**, 488 (1970)

Virk, P. S., "An Elastic Sublayer Model for Drag Reduction by Dilute Solutions of Linear Macromolecules", *JFM*, **45**, 417 (1971)

Virk, P. S., "Drag Reduction Fundamentals", *AICHE J.*, **21**, 625 (1975)

Walsh, M., Ph.D. Dissertation, Calif. Inst. Tech., Pasadena, CA (1967)

Zakin, J. L., and D. L. Hunston, "Effect of Polymer Molecular Variables on Drag Reduction, *J. Macromol. Sci.- Phys.*, **B18**, 795 (1980)

Zimm, B. H., *Journal of Physical Chemistry*, **24**, 269 (1956)

APPENDIX

Figure A-1 Intrinsic Viscosity Measurement
PSF-128 (MW=1090000)

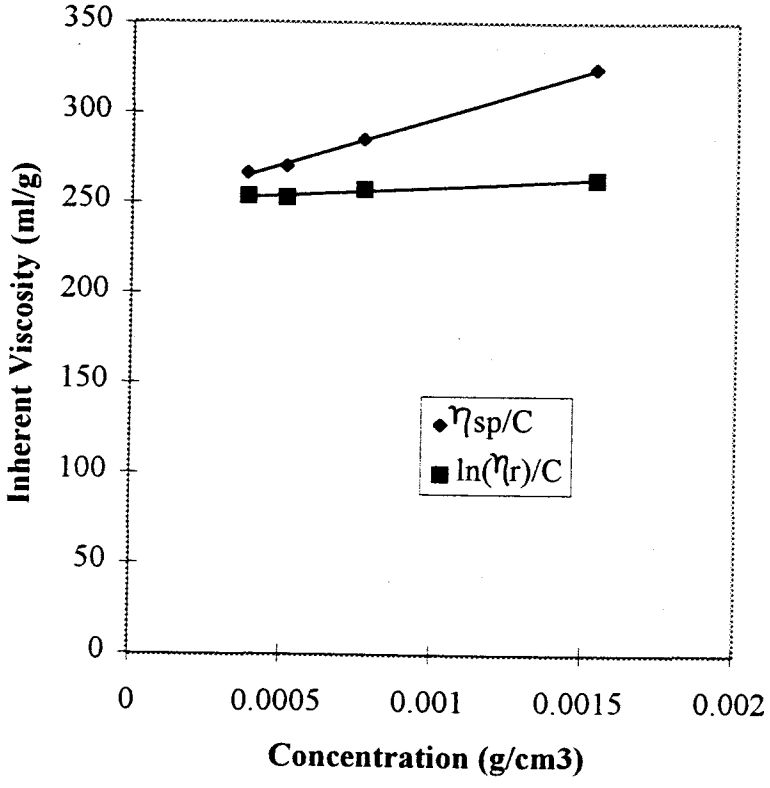

Figure A-2 Intrinsic Viscosity Measurement
PS-14A (MW=1650000)

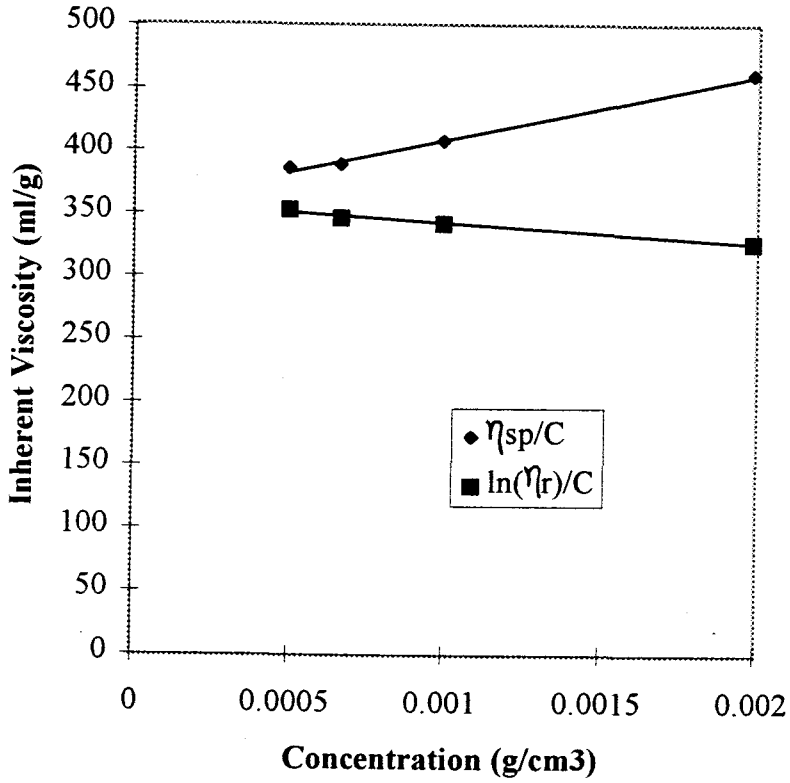

Figure A-3 Intrinsic Viscosity Measurement
PSF-380 (MW=3840000)

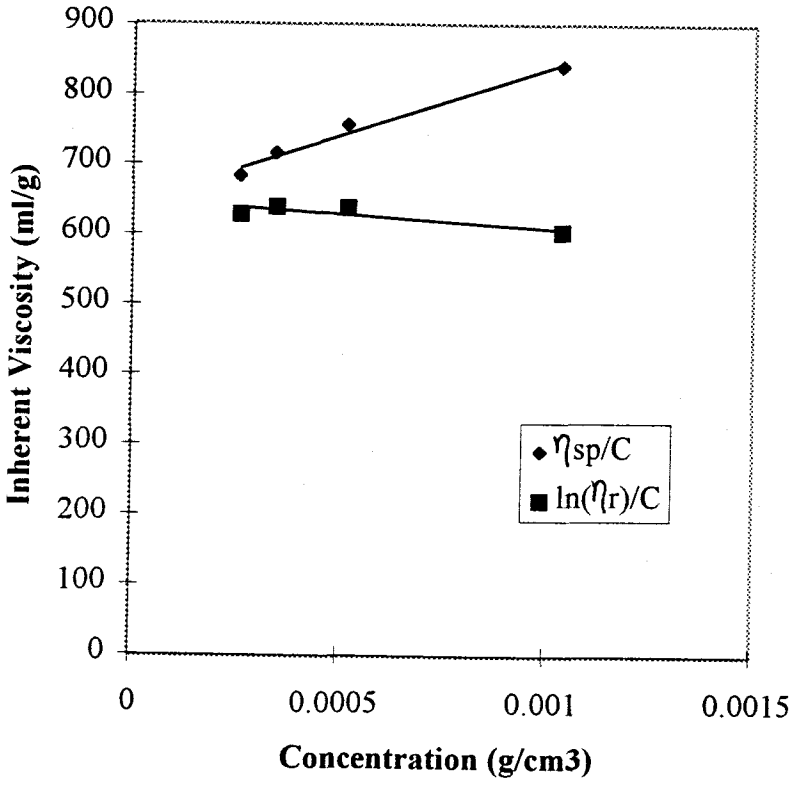

Figure A-4 Intrinsic Viscosity Measurement
PSF-550 (MW=5480000)

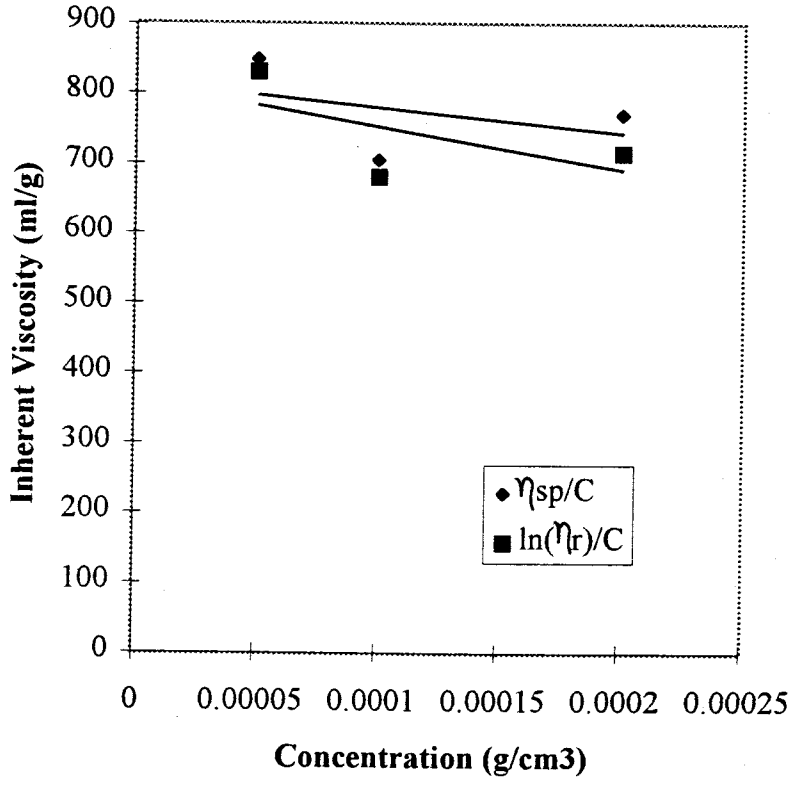

Figure A-5 Intrinsic Viscosity Measurement
PSF-850 (MW=8420000)

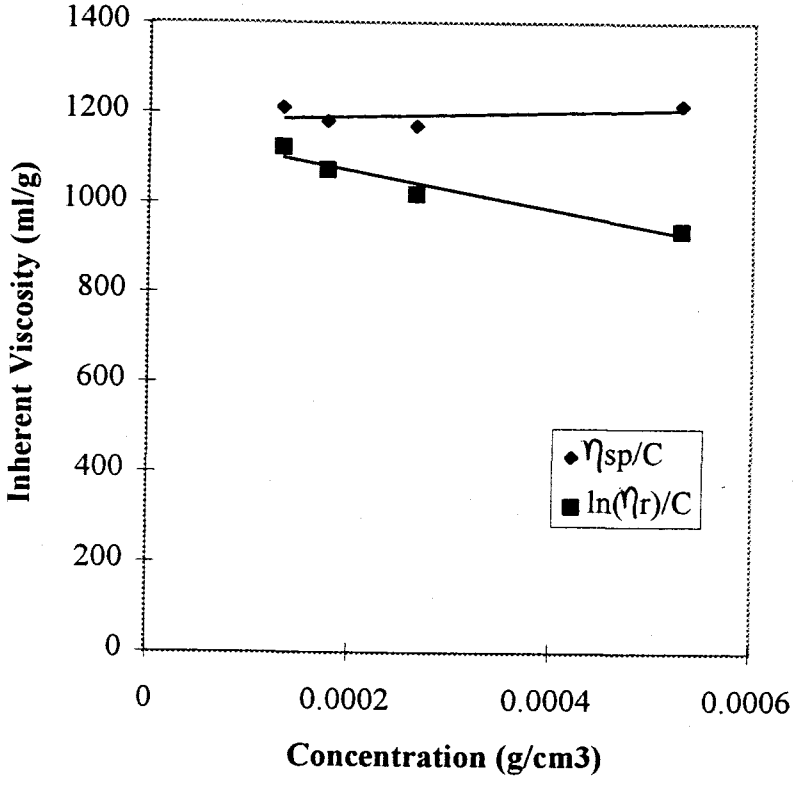

Figure A-6 Intrinsic Viscosity Measurement
PSF-2000 (MW=20000000)